

Supporting Information

Molecular Design of Benzothienobenzothiophene-Cored Columnar Mesogens: Facile Synthesis, Mesomorphism, and Charge Carrier Mobility

Chun-Xia Liu,¹ Hu Wang,¹ Jun-Qi Du,¹ Ke-Qing Zhao^{*,1} Ping Hu,¹ Bi-Qin Wang,¹ Hirosato Monobe^{*,2} Benoit Heinrich,³ Bertrand Donnio^{*,3}

1. College of Chemistry and Material sciences, Sichuan Normal University, Chengdu 610066, China. E-mail: kqzhao@sicnu.edu.cn
2. Inorganic Functional Materials Research Institute, National Institute of Advanced Industrial Science and Technology (AIST), Ikeda, Osaka 5638577, Japan. E-mail: monobe-hirosato@aist.go.jp
3. Institut de Physique et Chimie des Matériaux de Strasbourg (IPCMS), CNRS-Université de Strasbourg (UMR 7504), 23 rue du Loess, BP 43, 67034 Strasbourg Cedex 2 (France), E-mail: bertrand.donnio@ipcms.unistra.fr

Table of contents		
No.	Contents	Page No.
1	Experimental techniques	1
2	Synthesis and Characterization	2-5
3	POM photographs	6-7
4	DSC and TGA curves	8-11
5	SAXS indexation and patterns	12-14
6	TOF data and POM photos in cell	15-16
7	¹ H NMR spectra	17-26
8	HRMS spectra	26-28

1. Experimental techniques

Elemental analysis. EA were measured on a Vario Micro Select (Elementar company, German).

NMR, MS, UV-Vis, PL. ^1H NMR was measured on a Varian INOVA 400 MHz spectrometer in CDCl_3 using TMS as the internal standard. The high-resolution mass spectra (HRMS) were measured on a Fourier Transform ion cyclotron resonance mass spectrometer (7.0T FTICR-MS) instrument made by Ion Spec (Varian now) with MALDI or ESI as the ion source. Ultraviolet-visible (UV-Vis) absorption spectra were measured at room temperature on a Perkin Elmer Lambda 950 spectrophotometer. Photoluminescence (PL) was measured on a HORIBA Fluoromax-4p, and the absolute quantum yields were measured by a HORIBA-F-3029 Integrating Sphere, HORIBA, Kyoto, Japan.

POM, DSC and TGA. The optical textures of liquid crystals were observed using a XP-201 and an Olympus BH2 Polarised Optical Microscope (POM) equipped with a XP-201 and Mettler FP82HT hot-stages of which temperatures were controlled by a XPR-201 and Mettler FP90. The phase transition temperatures and enthalpies were investigated using a TA-DSC Q100 differential scanning calorimeter (DSC) under N_2 atmosphere with heating or cooling rate of 5-10 $^\circ\text{C}/\text{min}$. The thermal gravimetrical analysis (TGA) was measured on a TA TGA-Q500 instrument with heating rate of 20 $^\circ\text{C}/\text{min}$ in N_2 atmosphere.

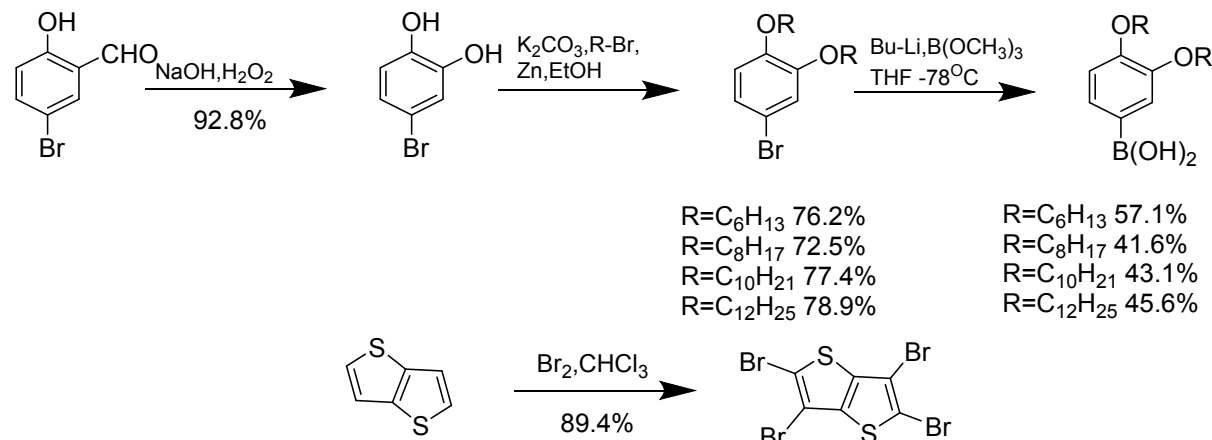
SAXS. Temperature-variation SAXS experiments were performed on a Rigaku Smartlab (3) X-Ray diffractometer equipped with a TCU 110 temperature control unit. The sample temperature was controlled within ± 1 K. The X-ray sources ($\text{Cu K}\alpha$, $\lambda = 0.154$ nm) were provided by 40 kW ceramic tubes.

TOF mobility. Electron and hole mobilities were measured by a TOF (time-of-flight) technique using a N_2 gas laser (KEN-1520, Usho, 600 ps pulse width, $\lambda = 337$ nm) and a hot stage. The cell with indium-tin-oxide (ITO) electrodes was mounted on a handmade hot stage, and electric bias was applied by dry cell batteries. Depending on the polarity of the applied electric field (20 to 50 kV/cm), positive or negative charge carriers were moving through the sample, causing displacement photocurrent, which was detected on a digital oscilloscope (DSO5052A, Agilent Technology) with a commercially available current amplifier (DHPCA-100, FEMTO). Thickness of the cell used for measurements was in range of 15-20 μm . The cells were filled with the material in its isotropic liquid state by capillary forces, and then cooled down to the hexagonal columnar phase. POM images showed a low birefringent

textures with homeotropic domains, and the laser focused on a spot with homeotropic aligned sample area.

2. Synthesis and characterization

All solvents and chemical reagents are commercial products, and were used without further purification.



Scheme S1. Syntheses of the arylboronic acids and of tetrabromobithiophene.

The syntheses of the precursory arylboronic acids [1] (Scheme S1), tetrabromobithiophene [2] (Scheme S1), and 2-bromobiphenyl [3] (**1-1**, Scheme 1) were performed according to reported methods. The synthesis of the fused thiophene[3,2-b]thiophene H-shaped liquid crystals (**M1-5**) and their precursors (**D2-5**), Scheme 1, is described below.

1-2 (Suzuki coupling): Under argon atmosphere, 2-bromobiphenyl **1-1** (300 mg, 0.594 mmol) [3], thiophene[3,2-b]thiophene-2-boronic acid (99.4 mg, 0.54 mmol), K_2CO_3 (1.12 g, 8.1 mmol), and $\text{Pd}(\text{PPh}_3)_4$ (49.7 mg, 0.043 mmol) were added to a reaction tube. The degassed mixed solution of H_2O (2 mL) and THF (10 mL) was injected, and the mixture heated to 80°C with stirring for 12 h. Once cooled, the mixture was extracted with CH_2Cl_2 and dried with MgSO_4 , solvent was evaporated by vacuum, and the residue purified by silica gel column chromatography with elution of light petroleum/ CH_2Cl_2 1:1 (vol) to yield the oil **1-2** (284 mg, 75 %). ^1H NMR (CDCl_3 , TMS, 400 MHz) δ : 7.25(d, J = 3.6 Hz, 1H, ArH), 7.13(d, J = 5.2 Hz, 1H, ArH), 7.06 (s, 1H, ArH), 6.90 (s, 1H, ArH), 6.85 (s, 1H, ArH), 6.81 (s 2H, ArH), 6.75 (s, 1H, ArH), 4.03~4.07 (m, 4H, OCH_2), 3.98 (t, J = 6.8 Hz, 2H, OCH_2), 3.72 (t, J = 6.8 Hz, 2H, OCH_2), 1.80~1.87 (m, 6H, CH_2), 1.58~1.63 (m, 2H, CH_2), 1.37~1.49 (m, 12H, CH_2), 1.24~1.30 (m, 4H, CH_2), 0.85~0.95 (m, 12H, CH_3).

1-3 (cyclodehydrogenation reaction): To a stirred solution of **1-2** (270 mg, 0.424 mmol) in CH_2Cl_2 (30 mL), FeCl_3 (138 mg, 0.848 mmol) in MeNO_2 (1.5 mL) was added and stirred at

[1] Zhang Q, Peng H, Zhang G, Lu Q, Chang J, Dong Y, Shi X, Wei J. *J. Am. Chem. Soc.*, 2014, 136, 5057-5064.

[2] Otsubo T, Kono Y, Hozo N, Miyamoto H, Aso Y, Ogura F, Tanaka T, Swada M. *Bull. Chem. Soc. Jpn.*, 1993, 66, 2033-2041.

[3] Zhao K Q, Du J Q, Long X H, Jing M, Wang B Q, Hu P, Monobe H, Henrich B, Donnio B. *Dyes Pigm.*, 2017, 143, 252-260.

room temperature for 1 h. Then, cold MeOH (3 mL) and water (3 mL) were added, and the product was extracted with CH₂Cl₂, dried with MgSO₄, the organic solvent evaporated under reduced pressure, the residue purified by silica gel column with elution of light petroleum/CH₂Cl₂ 1:1 (vol), and recrystallized in EtOAc/EtOH to yield the white crystalline solid **1-3** (217 mg, 81 %). ¹H NMR (CDCl₃, TMS, 400 MHz): δ: 7.92 (s, 1H, ArH), 7.87 (s, 1H, ArH), 7.77 (s, 1H, ArH), 7.56 (d, *J* = 5.2 Hz 1H, ArH), 7.46 (d, *J* = 5.2 Hz, 1H, ArH), 7.37 (s, 1H, ArH), 4.19~4.33 (m, 8H, OCH₂), 1.93~2.04 (m, 8H, CH₂), 1.42~1.64 (m, 16H, CH₂), 0.96~1.00 (m, 12H, CH₃).

D2 (Suzuki cross-coupling). Under an argon atmosphere, to the mixture of tetrabromothieno[3,2-b]thiophene (100 mg, 0.22 mmol), (3,4-(hexyloxy)phenyl)boronic acid (424.2 mg, 1.3 mmol), K₂CO₃ (1.2 g, 8.8 mmol), and Pd(PPh₃)₄ (101.4 mg, 0.09 mmol), was injected H₂O (5 mL) and THF (12 mL), and then was heated at 75°C for 36 h with stirring. Once cooled, the product was extracted with CH₂Cl₂, dried with MgSO₄, the organic solvent evaporated under vacuum, the residue purified by silica column chromatography with elution of light petroleum/dichloromethane 3:1 (vol), recrystallized in methanol-ethanol to yield a pale yellow solid **D2** (254 mg, 92.9 %). ¹H NMR (CDCl₃, TMS, 400 MHz) δ: 7.01 (d, *J* = 2.0 Hz, 1H, ArH), 6.99 (d, *J* = 2.0 Hz, 1H, ArH), 6.98 (d, *J* = 2.0 Hz, 2H, ArH), 6.91 (d, 1H, *J* = 2.0 Hz, ArH), 6.89 (d, *J* = 2.0 Hz, 1H, ArH), 6.87 (s, 1H, ArH), 6.85 (s, 3H, ArH), 6.78 (s, 1H, ArH), 6.76 (s, 1H, ArH), 3.95~4.02 (m, 8H, OCH₂), 3.84 (t, *J* = 6.8 Hz, 4H, OCH₂), 3.76 (t, *J* = 6.8 Hz, 4H, OCH₂), 1.81~1.85 (m, 8H, CH₂), 1.67~1.79 (m, 8H, CH₂), 1.43~1.48 (m, 8H, CH₂), 1.32~1.35 (m, 24H, CH₂), 1.28~1.34 (m, 16H, CH₂), 0.87~0.91 (m, 24H, CH₃).

D3 to **D5** were synthesized according to the same procedure used for **D2**

D3: Tetrabromothieno[3,2-b]thiophene (100 mg, 0.22 mmol), (3,4-(octyloxy)phenyl)boronic acid (498.1 mg, 1.32 mmol), Pd(PPh₃)₄ (101.4 mg, 0.09 mmol). **D3:** 243.8 mg, 75.6 %. ¹H NMR (CDCl₃, TMS, 400 MHz) δ: 7.01 (d, *J* = 2.0 Hz, 1H, ArH), 6.99 (d, *J* = 2.0 Hz, 1H, ArH), 6.97 (d, *J* = 2.0 Hz, 2H, ArH), 6.91 (d, *J* = 2.0 Hz, 1H, ArH), 6.89 (d, *J* = 2.0 Hz, 1H, ArH), 6.86 (s, 1H, ArH), 6.84 (s, 3H, ArH), 6.78 (s, 1H, ArH), 6.76 (s, 1H, ArH), 3.95~4.02 (m, 8H, OCH₂), 3.83 (t, *J* = 6.8 Hz, 4H, OCH₂), 3.76 (t, *J* = 6.8 Hz, 4H, OCH₂), 1.77~1.85 (m, 8H, CH₂), 1.67~1.74 (m, 8H, CH₂), 1.43~1.48 (m, 8H, CH₂), 1.28~1.37 (m, 64H, CH₂), 1.25~1.27 (m, 8H, CH₂), 0.87~0.89 (m, 24H, CH₃).

D4: Tetrabromothieno[3,2-b]thiophene (150 mg, 0.33 mmol), (3,4-(decyloxy)phenyl)boronic acid (857.8 mg, 1.97 mmol), Pd(PPh₃)₄ (152.2 mg, 0.09 mmol). **D4:** 411 mg, 73.0 %. ¹H NMR (CDCl₃, TMS, 400 MHz) δ: 7.01 (d, *J* = 1.6 Hz, 1H, ArH), 6.99 (s, 1H, ArH), 6.97 (d, *J* = 2.0 Hz, 2H, ArH), 6.91 (d, *J* = 2.0 Hz, 1H, ArH), 6.89 (d, *J* = 1.6 Hz, 1H, ArH), 6.86 (s, 1H, ArH), 6.84 (d, *J* = 2.4 Hz, 3H, ArH), 6.78 (s, 1H, ArH), 6.76 (s, 1H, ArH), 3.95~4.02 (m, 8H, OCH₂), 3.83 (t, *J* = 6.4 Hz, 4H, OCH₂), 3.75 (t, *J* = 6.4 Hz, 4H, OCH₂), 1.79~1.85 (m, 8H, CH₂), 1.67~1.74 (m, 8H, CH₂), 1.45~1.48 (m, 8H, CH₂), 1.27~1.43 (m, 104H, CH₂), 0.86~0.88 (m, 24H, CH₃).

D5: Tetrabromothieno[3,2-b]thiophene (150 mg, 0.33 mmol), (3,4-(dodecyloxy)phenyl)boronic acid (967.6 mg, 1.97 mmol), Pd(PPh₃)₄ (152.2 mg, 0.09 mmol). **D5:** 405 mg, 62.3 %. ¹H NMR (CDCl₃, TMS, 400 MHz) δ: 7.01 (d, *J* = 2.0 Hz, 1H, ArH), 6.99 (d, *J* = 1.6 Hz, 1H, ArH), 6.97 (d, *J* = 2.0 Hz, 2H, ArH), 6.91 (d, *J* = 2.0 Hz, 1H, ArH), 6.89 (d, *J* = 2.0 Hz, 1H, ArH), 6.86 (s, 1H, ArH), 6.84 (d, *J* = 2.0 Hz, 3H, ArH), 6.78 (s, 1H, ArH), 6.76 (s, 1H, ArH), 3.95~4.02 (m, 8H, OCH₂), 3.83 (t, *J* = 6.8 Hz, 4H, OCH₂), 3.75 (t, *J* = 6.8 Hz, 4H, OCH₂),

OCH₂), 1.81-1.86(m, 10H, CH₂), 1.68-1.76(m, 6H, CH₂), 1.43-1.46(m, 10H, CH₂), 1.26-1.36(m, 132H, CH₂), 0.88(t, *J* = 4.8 Hz, 24H, CH₃).

M1 was synthesized by intermolecular cyclodehydrogenation (cross oxidation). To a solution of **1-3** (78 mg, 0.157 mmol) and 3,3',4,4'-tetra(pentyloxy)-1,1-biphenyl (100 mg, 0.157 mmol) in CHCl₃ (25 mL), were added with stirring FeCl₃ (102.6 mg, 0.63 mmol) in MeNO₂ (1 mL). After 1 h, cold MeOH (2 mL) and H₂O (2 mL) were added. It was extracted by CHCl₃, dried with MgSO₄, organic solvent evaporated under vacuum, the residue purified by silica column with elution of light petroleum/ethyl acetate/CHCl₃ 10:20:0.3 (vol), and recrystallized from EtOAc-EtOH to get a white solid **M1** (80 mg, 45 %). ¹H NMR (CDCl₃, TMS, 400 MHz) δ: 8.07 (s, 2H, ArH), 8.00 (s, 2H, ArH), 7.95 (s, 2H, ArH), 7.48 (s, 2H, ArH), 4.31 (t, *J* = 6.4 Hz 4H, CH₂), 4.11~4.18 (m, 8H, CH₂), 3.99 (t, *J* = 6.0 Hz, 2H, OCH₂), 1.87~1.97 (m, 16H, CH₂), 1.39~1.61 (m, 32H, CH₂), 0.95~1.04 (m, 24H, CH₃). HRMS m/z (100%) (ESI): [M]⁺ Calcd for C₇₀H₉₆O₈S₂ 1128.6545, Found: 1128.6545. Elemental analysis: Calcd for C₇₀H₉₆O₈S₂: C, 74.43%; H, 8.57%; S, 5.68%. Found: C, 74.27%; H, 8.38%; S, 5.34%.

M2 was synthesized by intramolecular cyclodehydrogenation. To a stirred solution of **D2** (200 mg, 0.16 mmol) in CH₂Cl₂ (40 mL), were added FeCl₃ (156.2 mg, 0.96 mmol) in MeNO₂ (3.0 mL). After 2 h stirring, solids were deposited. Cold MeOH and water were added, solid was filtrated, washed 3 times with water and methanol. The filtrate was recrystallized in toluene-light petroleum to yield a pale solid **M2** (199.3 mg, 82.5%). ¹H NMR (CDCl₃, TMS, 400 MHz) δ: 7.95-7.97(m, 6H, ArH), 7.51-7.56(m, 2H, ArH), 4.43(t, *J* = 6.4 Hz, 4H, OCH₂), 4.30(t, *J* = 6.0 Hz, 12H, OCH₂), 2.03-2.09(m, 4H, CH₂), 1.96-2.02(m, 12H, CH₂), 1.68-1.73(m, 12H, CH₂), 1.44-1.49(m, 32H, CH₂), 0.95-0.99(m, 24H, CH₃). HRMS m/z (100%) (ESI): [M]⁺ calcd for C₇₈H₁₁₂O₈S₂ 1240.7799, found 1240.7795. Elemental analysis: Calcd for C₇₈H₁₁₂O₈S₂: C, 75.44%; H, 9.09%; S, 5.16%. Found: C, 74.28%; H, 8.87%; S, 4.95%.

M3 - M5 were synthesized according to the same procedure used for **M2**.

M3: D3 (100 mg, 0.07 mmol), FeCl₃ (66.2 mg, 0.41mmol). **M3:** 74.5mg, 74.7%. ¹H NMR (CDCl₃, TMS, 400 MHz) δ: 8.02(s, 2H, ArH), 7.96(s, 2H, ArH), 7.91 (s, 2H, ArH), 7.53(s, 2H, ArH), 4.44(t, *J* = 6.4 Hz, 4H, OCH₂), 4.30(t, *J* = 6.4 Hz, 12H, OCH₂), 2.04-2.10(m, 4H, CH₂), 1.96-2.03(m, 12H, CH₂), 1.68-1.71(m, 4H, CH₂), 1.61-1.69(m, 12H, CH₂), 1.45-1.49(m, 32H, CH₂), 1.27-1.44(m, 32H, CH₂), 0.88-0.94(m, 24H, CH₃). HRMS m/z (100%) (ESI): [M]⁺ calcd for C₉₄H₁₄₄O₈S₂ 1466.0336, found 1466.0331. Elemental analysis: Calcd for C₉₄H₁₄₄O₈S₂: C, 77.00%; H, 9.90%; S, 4.37%. Found: C, 77.13%; H, 9.92%; S, 3.98%.

M4: D4 (360 mg, 0.21 mmol), FeCl₃ (204.7 mg, 1.26 mmol). **M4:** 256 mg, 71.3%. ¹H NMR(CDCl₃, TMS, 400 MHz), δ: 8.00(s, 2H, ArH), 7.96(s, 2H, ArH), 7.91 (s, 2H, ArH), 7.53(s, 2H, ArH), 4.44(t, *J* = 6.8 Hz, 4H, OCH₂), 4.29(t, *J* = 6.8 Hz, 12H, OCH₂), 2.05-2.11(m, 4H, CH₂), 1.97-2.04(m, 12H, CH₂), 1.67-1.71(m, 4H, CH₂), 1.60-1.62(m, 12H, CH₂), 1.49-1.50(m, 24H, CH₂), 1.27-1.37(m, 72H, CH₂), 0.87-0.91(m, 24H, CH₃). HRMS m/z (100%) (ESI): [M]⁺ calcd for C₁₁₀H₁₇₆O₈S₂ 1690.2840, found 1690.2839. Elemental analysis: Calcd for C₁₁₀H₁₇₆O₈S₂: C, 78.14%; H, 10.49%; S, 3.79%. Found: C, 78.12%; H, 10.24%; S, 3.66%.

M5: D5 (150 mg, 0.08 mmol), FeCl₃ (73.8 mg, 0.45 mmol). **M5:** 125.6 mg, 83.9%. ¹H NMR (CDCl₃, TMS, 400 MHz) δ: 7.92-7.94(m, 6H, ArH), 7.49-7.51(m, 2H, ArH), 4.34-4.45(m, 4H, OCH₂), 4.22-4.34(m, 12H, OCH₂), 2.07-2.11(m, 6H, CH₂), 1.99-2.01(m, 12H, CH₂), 1.44-1.48(m, 18H, CH₂), 1.60-1.62(m, 12H, CH₂), 1.49-1.50(m, 24H, CH₂), 1.27-1.37(m, 72H, CH₂),

0.87-0.91(m, 24H, CH₃). HRMS m/z (100%) (ESI): [M+H]⁺ calcd for C₁₂₆H₂₀₈O₈S₂ 1914.5344, found 1915.5406. Elemental analysis: Calcd for C₁₂₆H₂₀₈O₈S₂: C, 79.02%; H, 10.95%; S, 3.35%. Found: C, 79.11%; H, 10.83%; S, 3.38%.

3. POM pictures

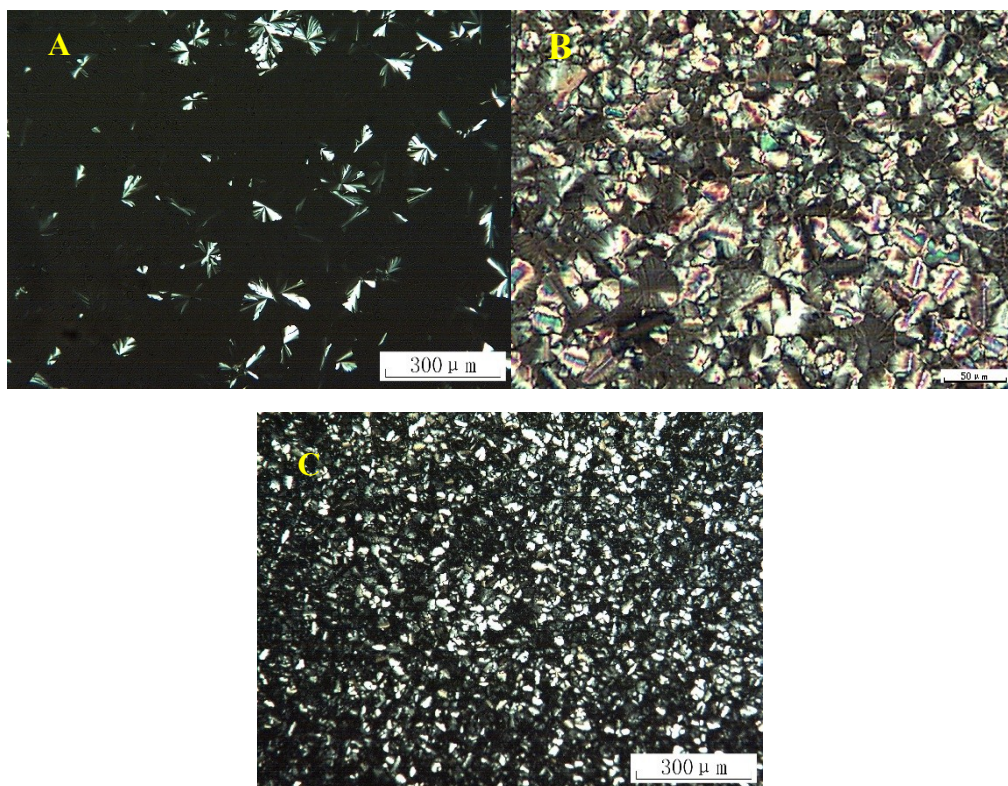
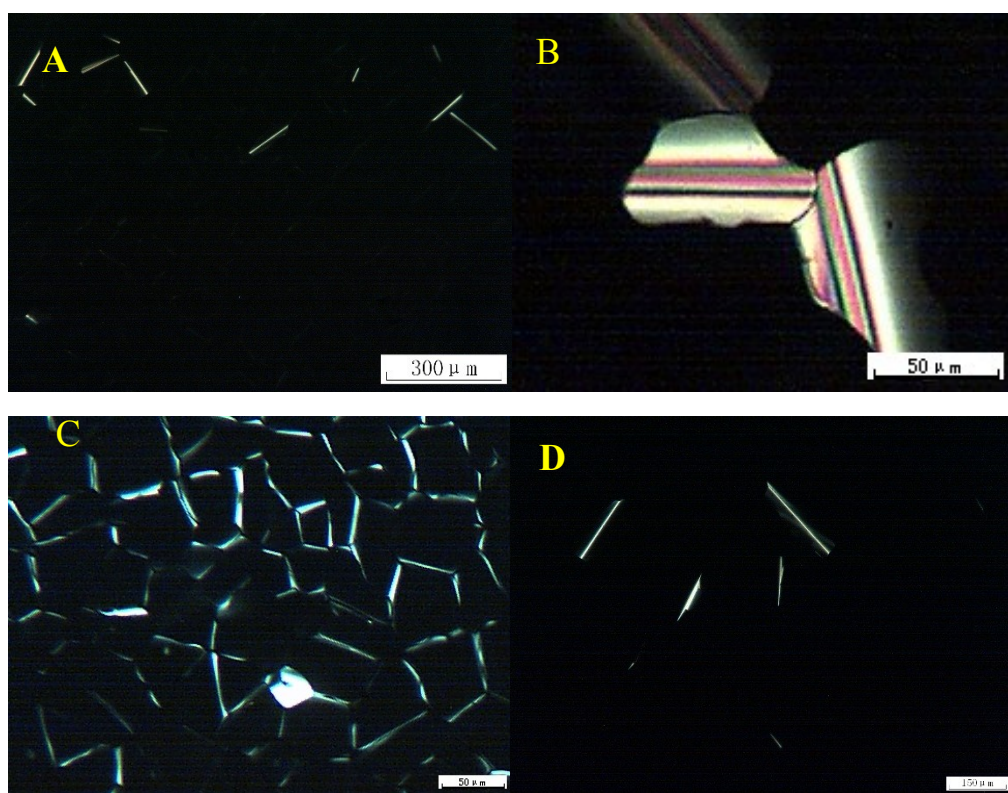


Figure S1. POM of intermediate tetraarylthiophenes in pseudo crystalline phases. A: **D3** at 66°C; B: **D4** at 45°C; C: **D5** at 32°C (see text).



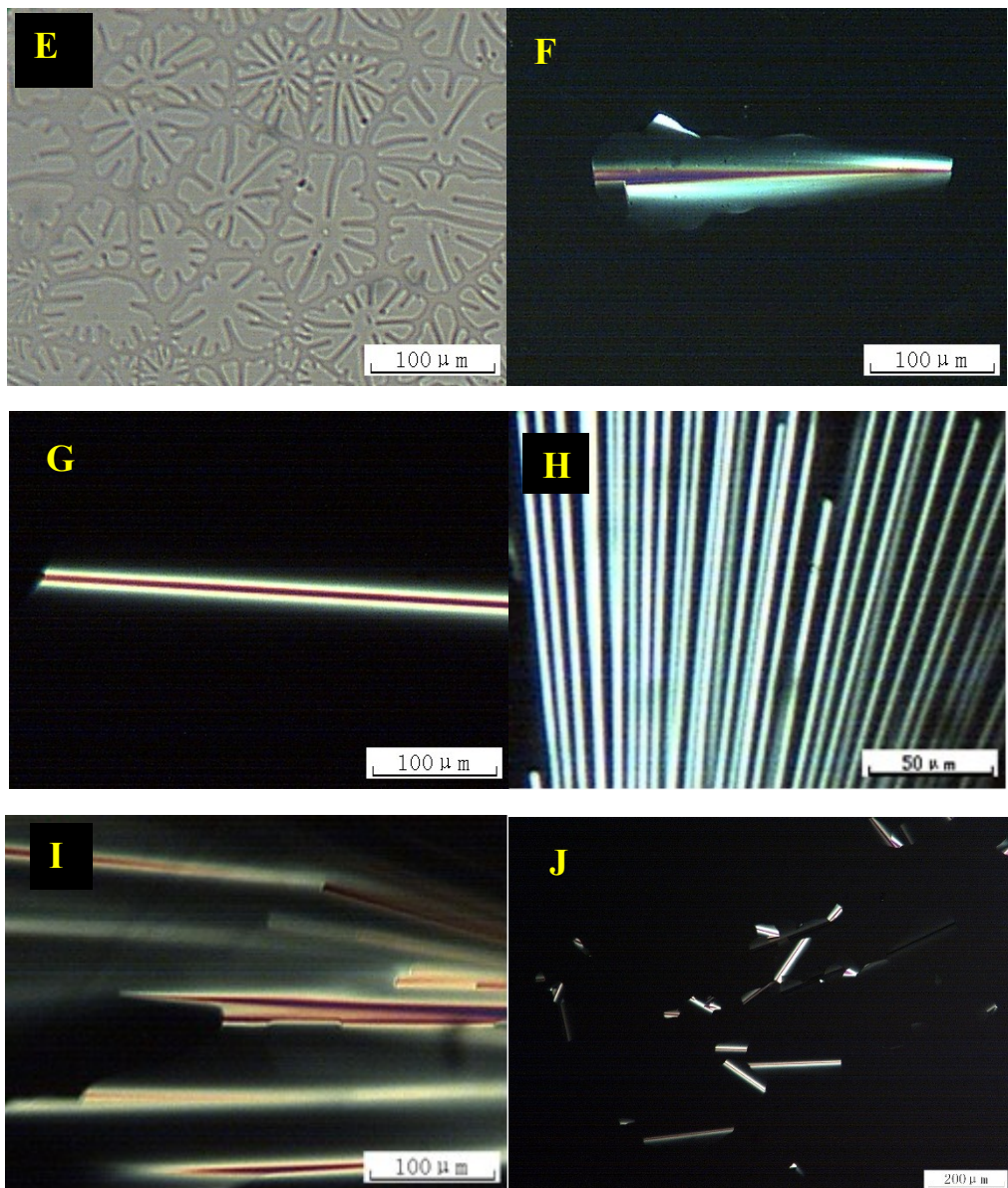
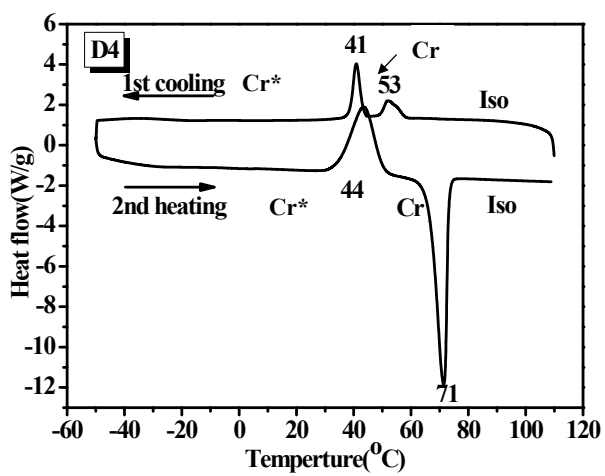
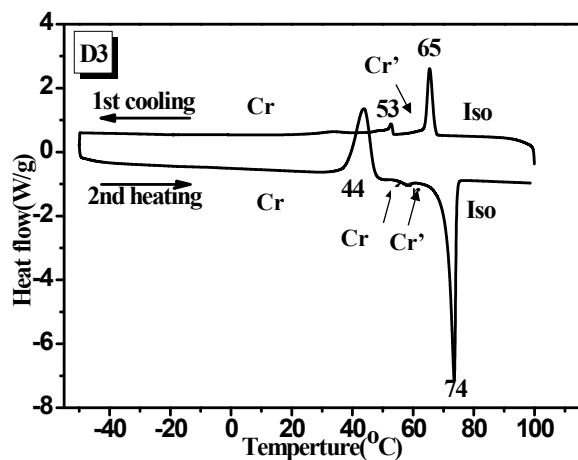
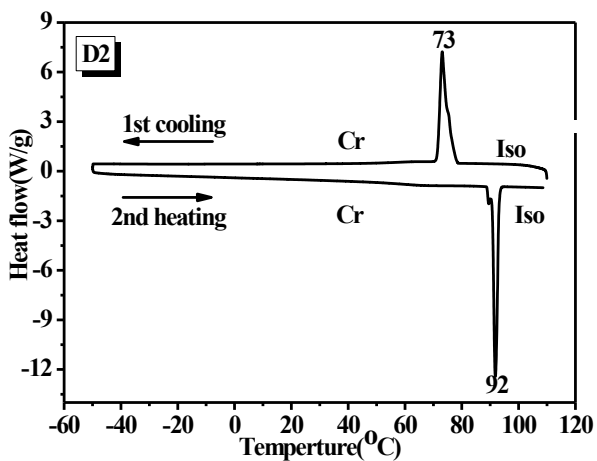


Figure S2. Polarising optical photomicrographs of the mesogens of series **M** show large homeotropic domains with straight defect lines and developable domains, in agreement with hexagonal columnar mesophases. Note the characteristic homeotropically grown hexagonal columnar domains in picture E. A: **M1** at 297°C; B,C: **M2** at 255 and 220°C; D,E,F: **M3** at 250, 284 and 256°C; G,H,I: **M4** at 248, 250 and 245°C; J: **M5** at 198°C.

4. DSC and TGA



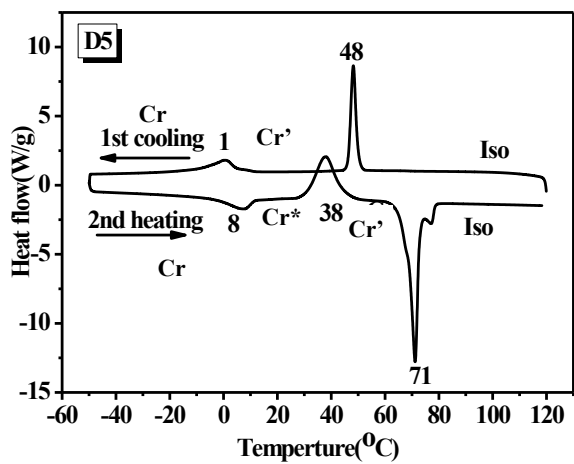
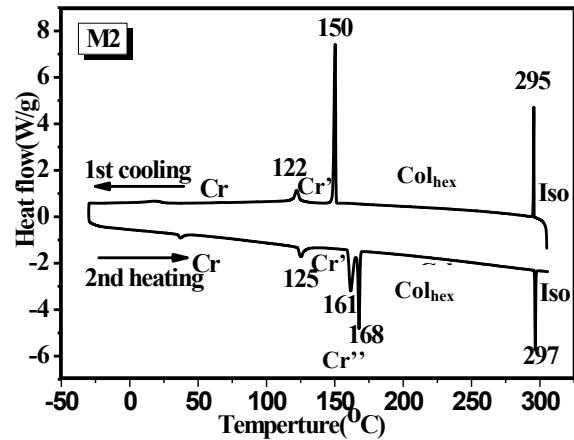
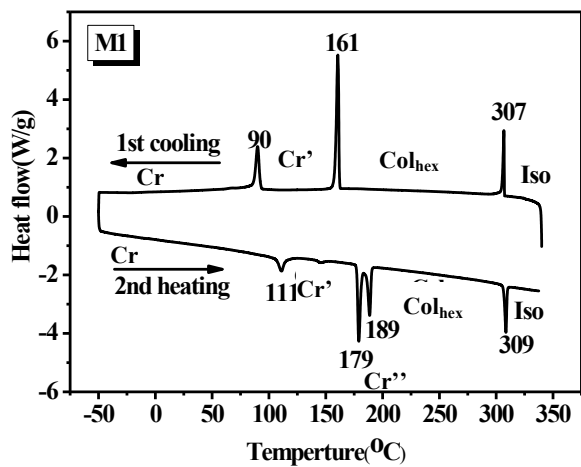


Figure S3. DSC curves of intermediate tetraarylthieno[3,2-b]thiophenes **D2-D5** (heating/cooling rate 5°C/min)



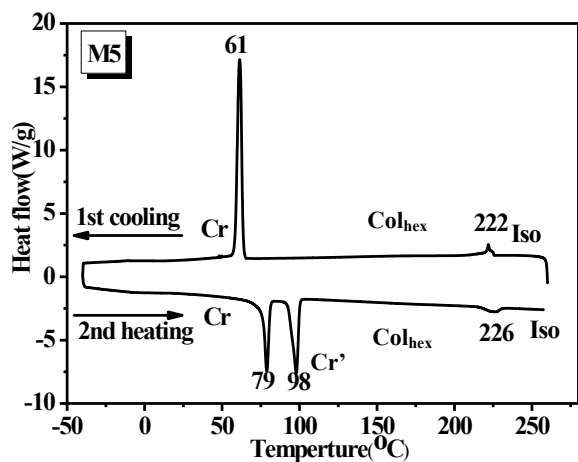
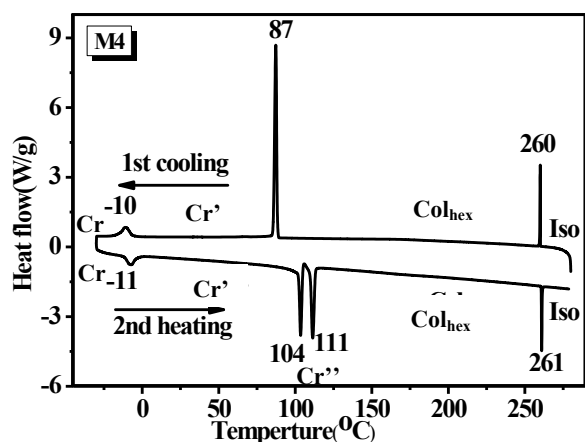
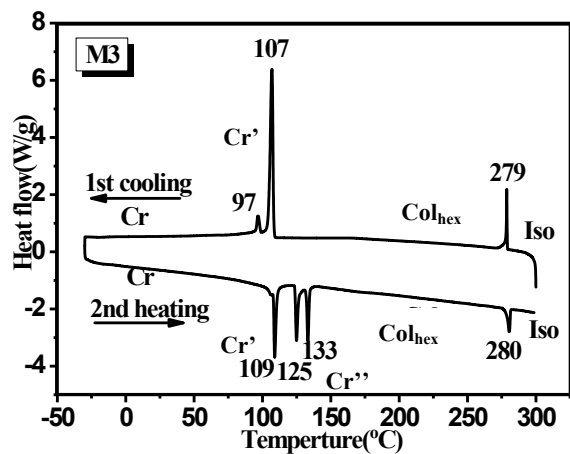


Figure S4. DSC curves of H-shaped columnar mesogens **M1-M5** (heating/cooling rate 5°C/min).

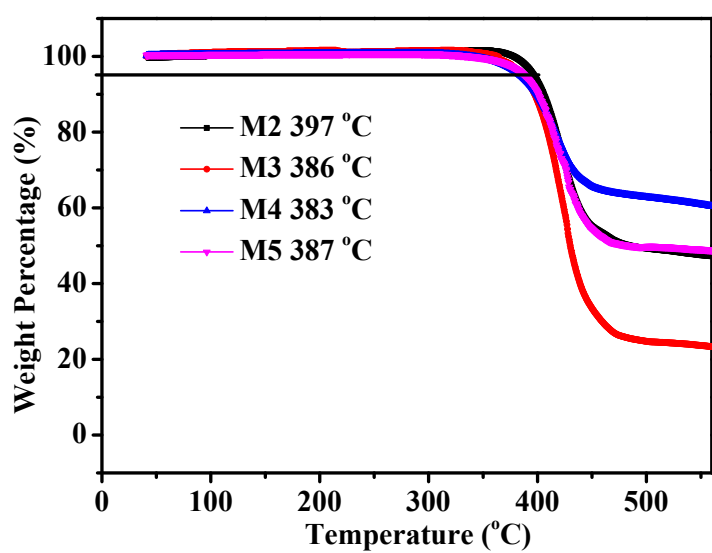


Figure S5. TGA curves. The temperatures shown in graph are the decomposition temperatures (5% weight loss temperature) of the compounds **M2-M5**.

5. SAXS

Table S1: Table of indexation†

	d _{meas} (Å) [sh;br/ξ(nm), Intensity]	(hk) Peak	d _{calc} (Å)	Mesophase parameters
M1 T = 240°C	20.32 [sh, VS] (11.73) [sh, M] 10.17 [sh, W] 7.67 (sh, W) 14.5 [$\xi=6$, S] 5.2 [$\xi=5$, W] 4.5 [br, VS] 3.76 [$\xi=5$, S]	10 11 20 21 D ₁ D ₂ h _{ch} h _π	20.32 (11.73) 10.16 7.68	a = 23.5 Å A = 478 Å ²
M2 T = 230°C	20.52 [sh, VS] (11.84) [sh, VW] 10.32 [sh, W] 7.75 [sh, W] 13.8 [$\xi=6$, M] 5.3 [$\xi=7$, M] 4.5 [br, VS] 3.82 [$\xi=3$, M]	10 11 20 21 D ₁ D ₂ h _{ch} h _π	20.55 (11.87) 10.28 7.77	a = 23.7 Å A = 488 Å ²
M3 T = 210°C	23.0 [sh, VS] 11.6 [sh, W] 13.8 [$\xi=6$, M] 5.3 [$\xi=6$, W] 4.5 [br, VS] 3.76 [$\xi=3$, S]	10 20 D ₁ D ₂ h _{ch} h _π	23.1 11.55	a = 26.7 Å A = 616 Å ²
M4 T = 200°C	24.45 [sh, VS] (14.12) [sh, W] 12.4 [sh, W] 13.8 [$\xi=8$, M] 5.4 [$\xi=7$, W] 4.5 [br, VS] 3.76 [$\xi=2$, S]	10 11 20 D ₁ D ₂ h _{ch} h _π	24.6 (14.21) 12.3	a = 28.4 Å A = 700 Å ²
M5 T = 180°C	27.09 [sh, VS] 15.68 [sh, M] 13.50 [sh, W] 13.8 [$\xi=6$, M] 5.2 [$\xi=6$, W] 4.5 [br, VS] 3.73 [$\xi=4$, VS]	10 11 20 D ₁ D ₂ h _{ch} h _π	27.08 15.64 13.54	a = 31.3 Å A = 847 Å ²

†d_{meas}, measured periodicities of the reflections from columnar lattice with indexation (hk) (Miller indices); “sh” and “br” stand for sharp reflections and broad scatterings; Intensity of reflections and scattering signals (VS: very strong, S: strong, M: medium, W: weak, VW: very weak), and associated correlation lengths ξ for signals from short-range correlated structure D_i and from lateral distances between molecular segments h_i; short-range correlated periodicities D₁ and D₂, and lateral distances between chains (h_{ch}), and face-to-face piled triphenylene rings (h_π); d_{calc}, calculated spacing from optimized lattice parameter; lattice parameter (a), lattice area (S).

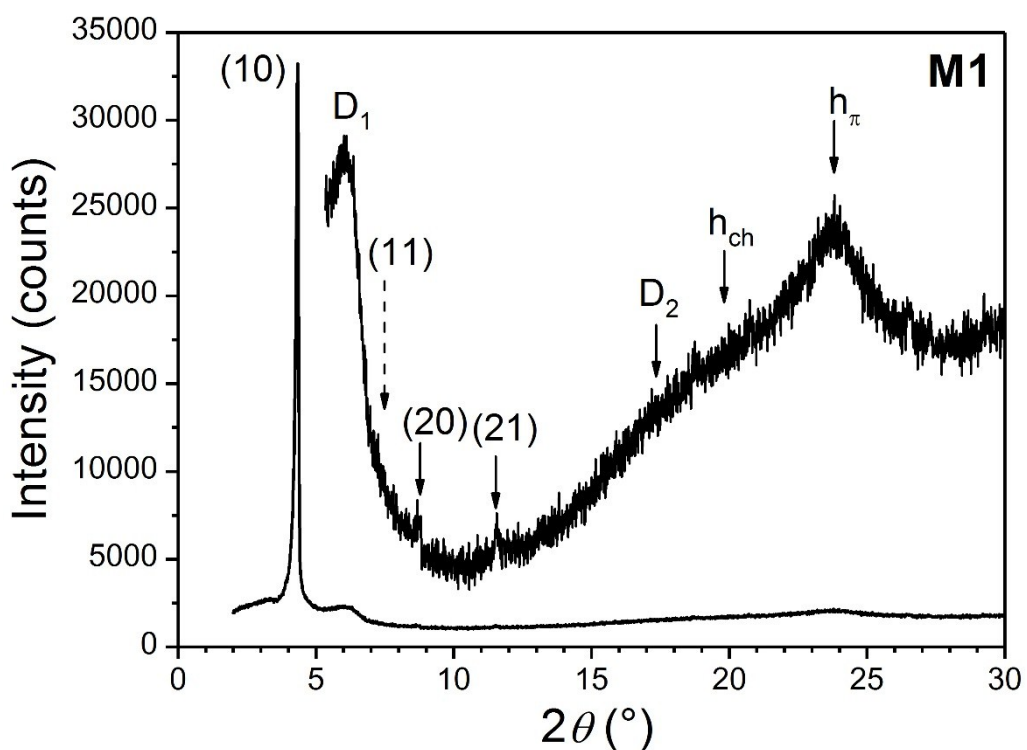


Figure S6. SAXS pattern of compound **M1** at 240°C.

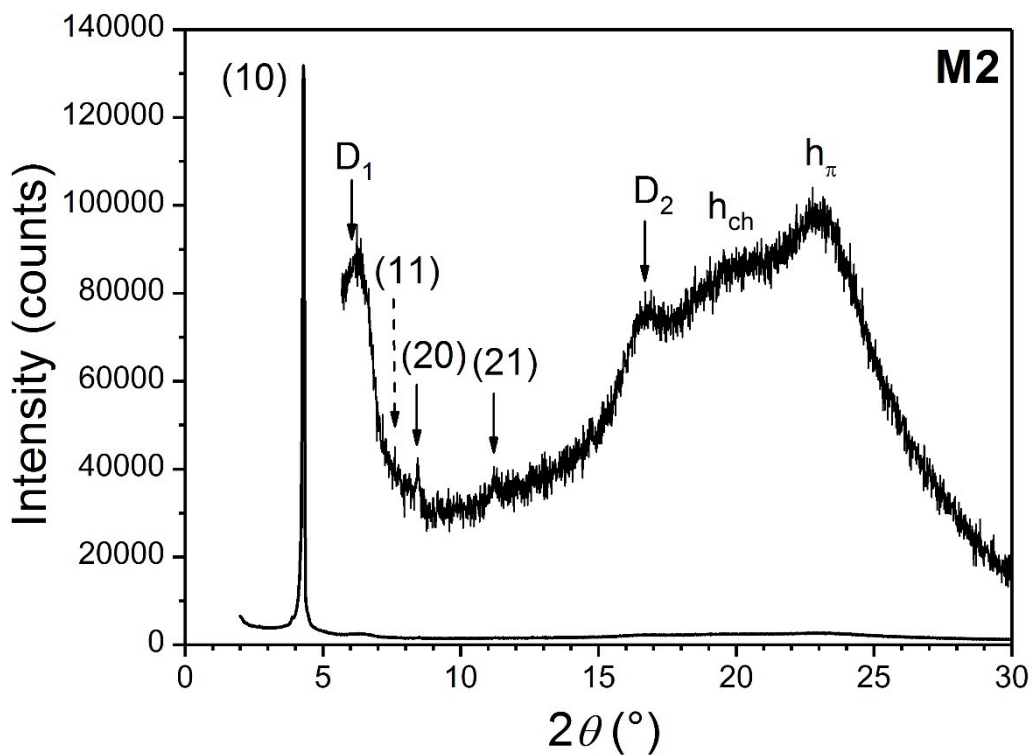


Figure S7. SAXS pattern of compound **M2** at 230°C.

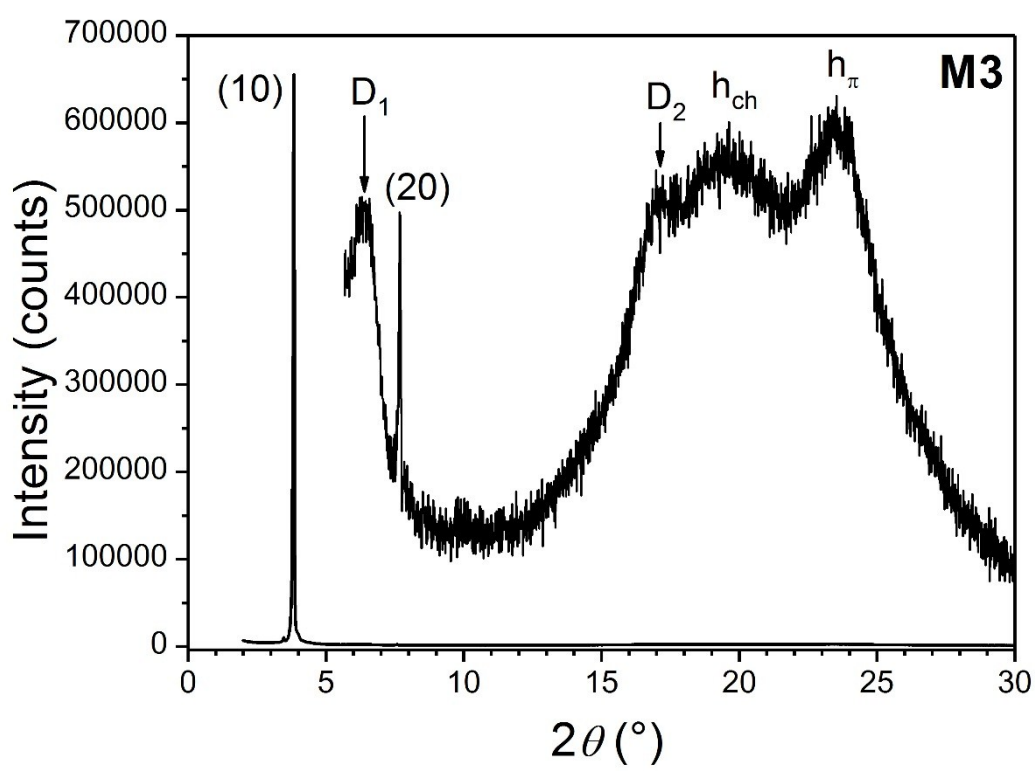


Figure S8. SAXS pattern of compound **M3** at 210°C.

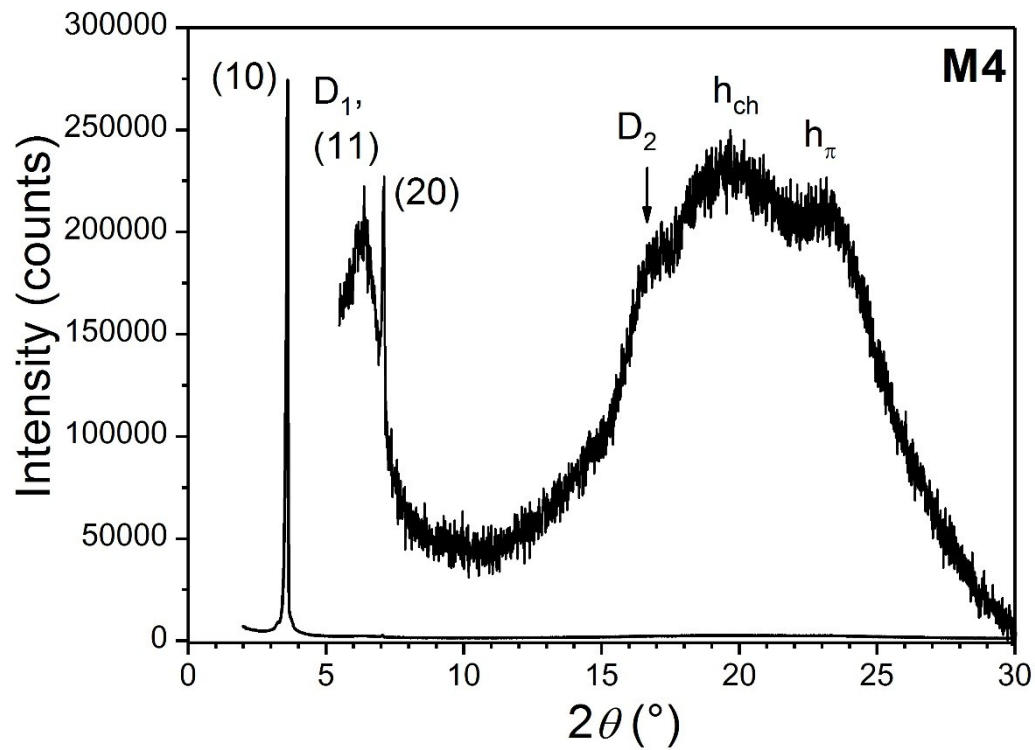


Figure S9. SAXS pattern of compound **M4** at 200°C.

6. TOF data and POM images in cell

Table S2: Electron and hole mobility at various temperatures and electric fields for mesogen **M4** (with liquid crystal cell thickness 16.4 μm)

Temperature /°C	Electric field/V	Transit time/s	Hole mobility/cm ² V ⁻¹ s ⁻¹	Transit time/s	Electron mobility/cm ² V ⁻¹ s ⁻¹
230	2×10^4	4.94×10^{-5}	1.66×10^{-3}	4.64×10^{-5}	1.77×10^{-3}
230	3×10^4	3.35×10^{-5}	1.63×10^{-3}	3.02×10^{-5}	1.81×10^{-3}
230	4×10^4	2.39×10^{-5}	1.71×10^{-3}	1.73×10^{-5}	2.37×10^{-3}
230	5×10^4	1.94×10^{-5}	1.69×10^{-3}	1.68×10^{-5}	1.95×10^{-3}
220	2×10^4	4.50×10^{-5}	1.82×10^{-3}	4.69×10^{-5}	1.75×10^{-3}
220	3×10^4	3.42×10^{-5}	1.60×10^{-3}	3.13×10^{-5}	1.75×10^{-3}
220	4×10^4	2.42×10^{-5}	1.70×10^{-3}	2.34×10^{-5}	1.75×10^{-3}
220	5×10^4	2.03×10^{-5}	1.61×10^{-3}	1.89×10^{-5}	1.73×10^{-3}
210	2×10^4	5.05×10^{-5}	1.62×10^{-3}	5.18×10^{-5}	1.58×10^{-3}
210	3×10^4	3.51×10^{-5}	1.56×10^{-3}	3.43×10^{-5}	1.59×10^{-3}
210	4×10^4	2.61×10^{-5}	1.57×10^{-3}	2.50×10^{-5}	1.64×10^{-3}
210	5×10^4	2.11×10^{-5}	1.55×10^{-3}	2.06×10^{-5}	1.59×10^{-3}
200	2×10^4	5.49×10^{-5}	1.49×10^{-3}	5.40×10^{-5}	1.52×10^{-3}
200	3×10^4	3.78×10^{-5}	1.45×10^{-3}	3.50×10^{-5}	1.56×10^{-3}
200	4×10^4	2.84×10^{-5}	1.44×10^{-3}	2.69×10^{-5}	1.52×10^{-3}
200	5×10^4	2.27×10^{-5}	1.44×10^{-3}	2.17×10^{-5}	1.51×10^{-3}
190	2×10^4	5.57×10^{-5}	1.47×10^{-3}	6.14×10^{-5}	1.34×10^{-3}
190	3×10^4	4.32×10^{-5}	1.27×10^{-3}	3.83×10^{-5}	1.43×10^{-3}
190	4×10^4	3.08×10^{-5}	1.33×10^{-3}	2.87×10^{-5}	1.43×10^{-3}
190	5×10^4	2.48×10^{-5}	1.32×10^{-3}	2.50×10^{-5}	1.31×10^{-3}
180	2×10^4	6.57×10^{-5}	1.25×10^{-3}	6.59×10^{-5}	1.24×10^{-3}
180	3×10^4	4.47×10^{-5}	1.22×10^{-3}	4.27×10^{-5}	1.28×10^{-3}
180	4×10^4	3.28×10^{-5}	1.25×10^{-3}	3.36×10^{-5}	1.22×10^{-3}
180	5×10^4	2.64×10^{-5}	1.24×10^{-3}	2.26×10^{-5}	1.23×10^{-3}
170	2×10^4	7.08×10^{-5}	1.16×10^{-3}	6.59×10^{-5}	1.23×10^{-3}
170	3×10^4	4.64×10^{-5}	1.18×10^{-3}	4.27×10^{-5}	1.19×10^{-3}
170	4×10^4	3.49×10^{-5}	1.17×10^{-3}	3.36×10^{-5}	1.24×10^{-3}
170	5×10^4	2.80×10^{-5}	1.17×10^{-3}	2.66×10^{-5}	1.22×10^{-3}
160	2×10^4	6.81×10^{-5}	1.20×10^{-3}	6.48×10^{-5}	1.27×10^{-3}
160	3×10^4	4.60×10^{-5}	1.19×10^{-3}	4.49×10^{-5}	1.22×10^{-3}
160	4×10^4	3.38×10^{-5}	1.21×10^{-3}	3.36×10^{-5}	1.22×10^{-3}
160	5×10^4	2.68×10^{-5}	1.22×10^{-3}	2.68×10^{-5}	1.22×10^{-3}
150	2×10^4	6.59×10^{-5}	1.24×10^{-3}	6.78×10^{-5}	1.21×10^{-3}
150	3×10^4	4.22×10^{-5}	1.29×10^{-3}	4.22×10^{-5}	1.30×10^{-3}
150	4×10^4	3.20×10^{-5}	1.28×10^{-3}	3.02×10^{-5}	1.36×10^{-3}
150	5×10^4	2.57×10^{-5}	1.27×10^{-3}	2.41×10^{-5}	1.36×10^{-3}
140	2×10^4	6.44×10^{-5}	1.27×10^{-3}		
140	3×10^4	4.13×10^{-5}	1.32×10^{-3}	3.72×10^{-5}	1.47×10^{-3}
140	2×10^4	3.09×10^{-5}	1.33×10^{-3}	2.88×10^{-5}	1.42×10^{-3}
140	3×10^4	2.44×10^{-5}	1.35×10^{-3}	2.44×10^{-5}	1.35×10^{-3}
130	2×10^4	6.36×10^{-5}	1.29×10^{-3}		
130	3×10^4	4.13×10^{-5}	1.32×10^{-3}	3.72×10^{-5}	1.47×10^{-3}
130	4×10^4	3.09×10^{-5}	1.33×10^{-3}	2.88×10^{-5}	1.42×10^{-3}
130	5×10^4	2.44×10^{-5}	1.35×10^{-3}	2.44×10^{-5}	1.35×10^{-3}
120	2×10^4	6.87×10^{-5}	1.19×10^{-3}	6.31×10^{-5}	1.30×10^{-3}
120	3×10^4	4.62×10^{-5}	1.18×10^{-3}	4.52×10^{-5}	1.21×10^{-3}
120	4×10^4	3.36×10^{-5}	1.22×10^{-3}	3.09×10^{-5}	1.33×10^{-3}
120	5×10^4	2.62×10^{-5}	1.25×10^{-3}	2.68×10^{-5}	1.23×10^{-3}
110	2×10^4	6.71×10^{-5}	1.22×10^{-3}	6.83×10^{-5}	1.20×10^{-3}
110	3×10^4	4.95×10^{-5}	1.10×10^{-3}	4.79×10^{-5}	1.14×10^{-3}
110	4×10^4	3.68×10^{-5}	1.11×10^{-3}	3.74×10^{-5}	1.10×10^{-3}

110	5×10^4	2.78×10^{-5}	1.18×10^{-3}	2.54×10^{-5}	1.29×10^{-3}
100	2×10^4	7.46×10^{-5}	1.10×10^{-3}	6.90×10^{-5}	1.19×10^{-3}
100	3×10^4	5.01×10^{-5}	1.09×10^{-3}	5.18×10^{-5}	1.05×10^{-3}
100	4×10^4	3.78×10^{-5}	1.08×10^{-3}	3.68×10^{-5}	1.11×10^{-3}
100	5×10^4	3.02×10^{-5}	1.09×10^{-3}	2.92×10^{-5}	1.12×10^{-3}

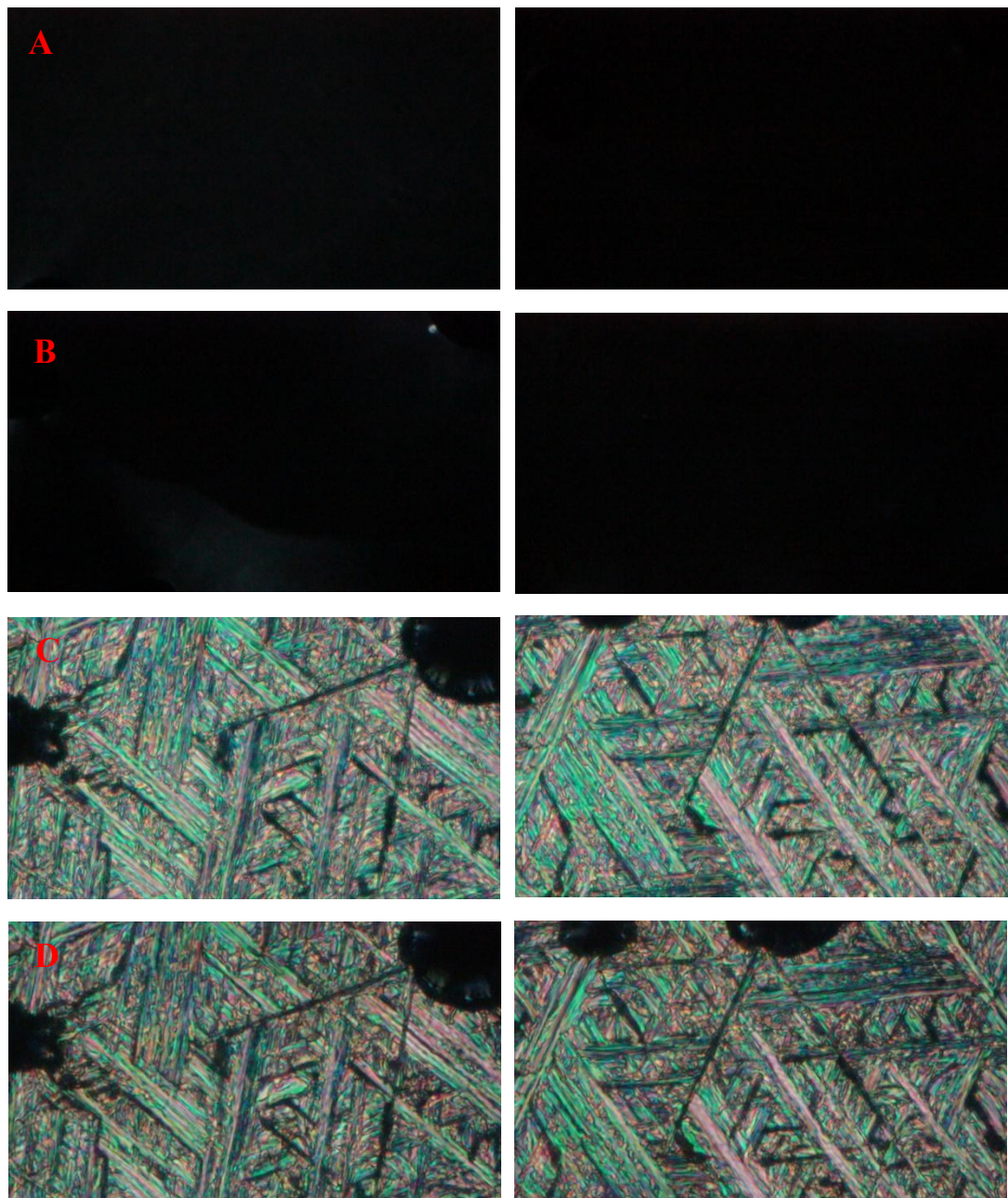


Figure S10. POM images taken during the TOF measurement (sample in ITO cell): A) Cooled to 220°C, and after rotating A&P by 45°(not stage rotation); B) Cooled to 120°C, and after rotating A&P by 45°(not stage rotation); C) Cooled to 80°C, and after rotating A&P by 45°(not stage rotation); D) Cooled to 27°C, and after rotating A&P by 45°(not stage rotation)

7. ^1H NMR

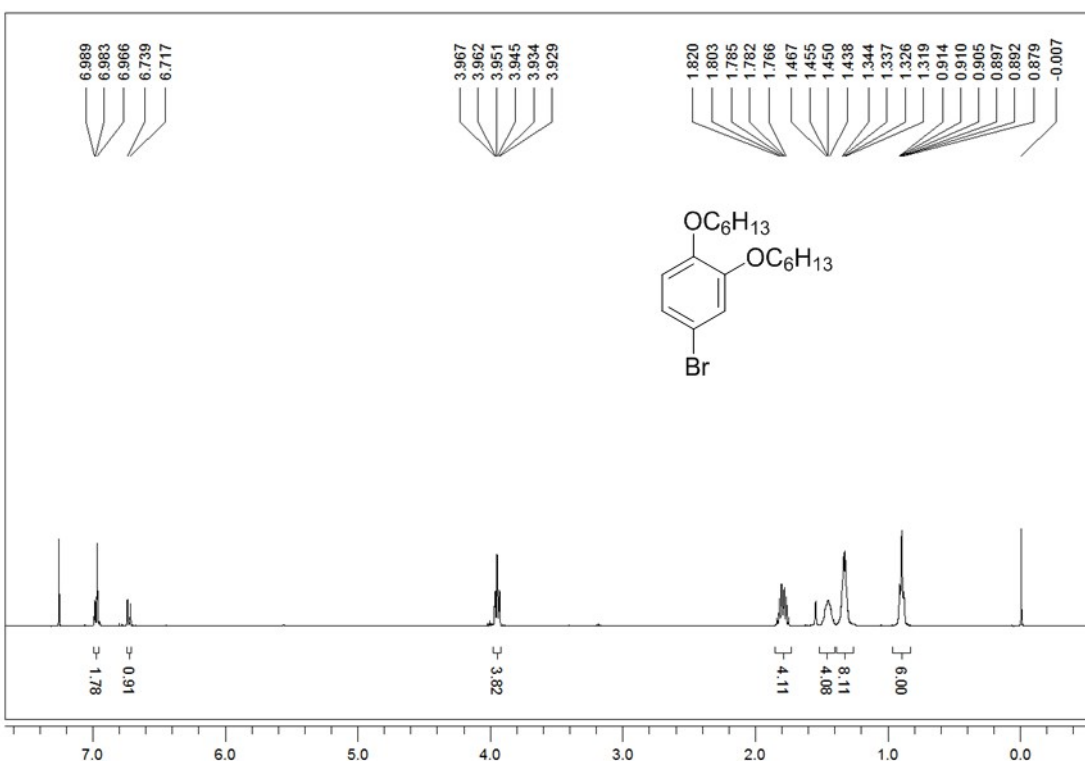


Figure S11. ^1H NMR (CDCl_3 , 400 MHz) spectrum of 4-bromo-1,2-bis(hexyloxy)benzene

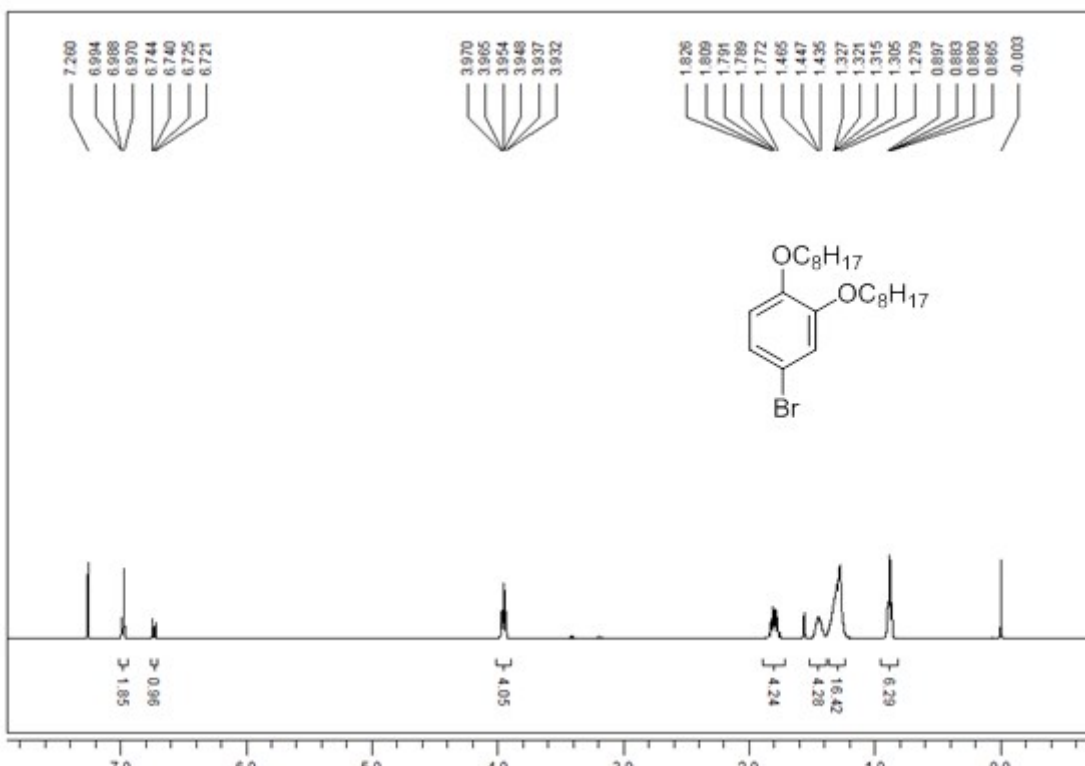


Figure S12. ^1H NMR (CDCl_3 , 400 MHz) spectrum of 4-bromo-1,2-bis(octyloxy)benzene

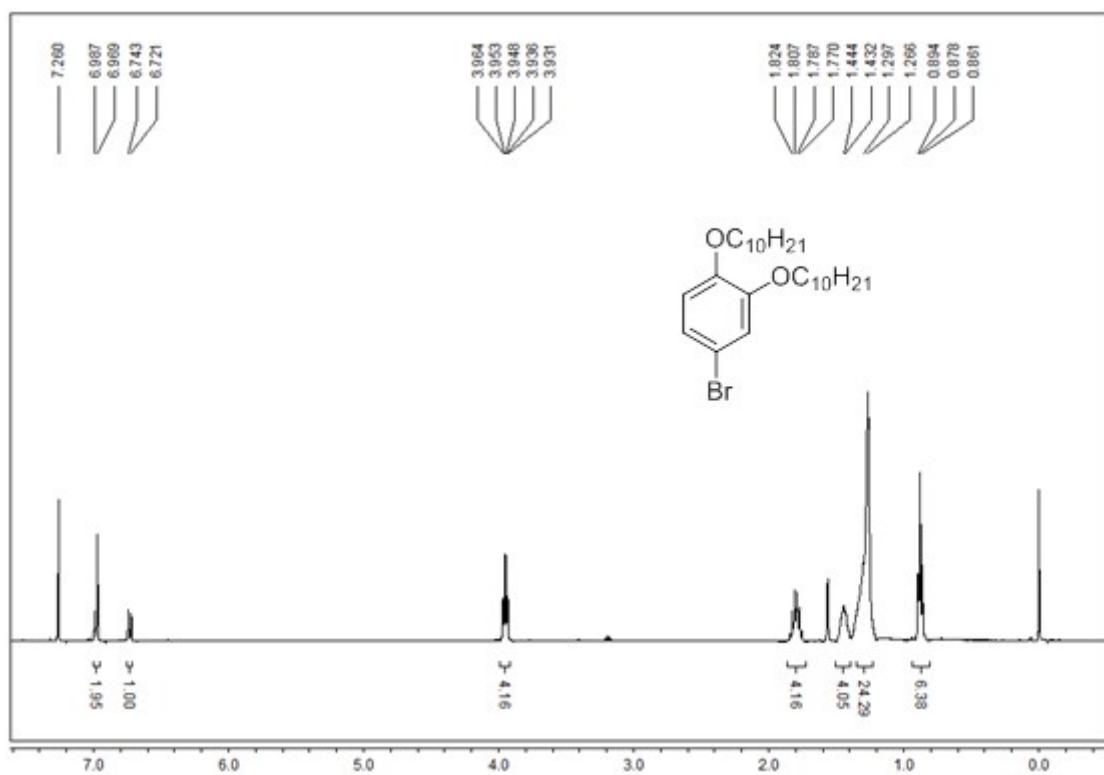


Figure S13. ^1H NMR (CDCl_3 , 400 MHz) spectrum of 4-bromo-1,2-bis(decyloxy)benzene

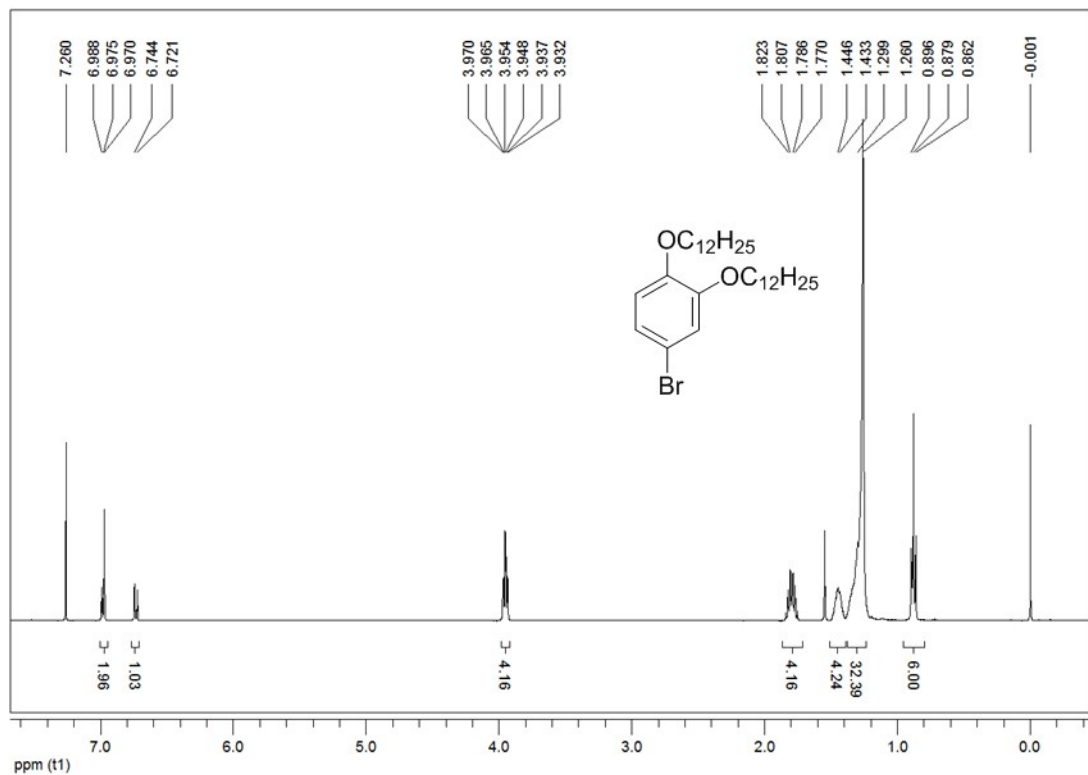


Figure S14. ^1H NMR (CDCl_3 , 400 MHz) spectrum of 4-bromo-1,2-bis(dodecyloxy)benzene

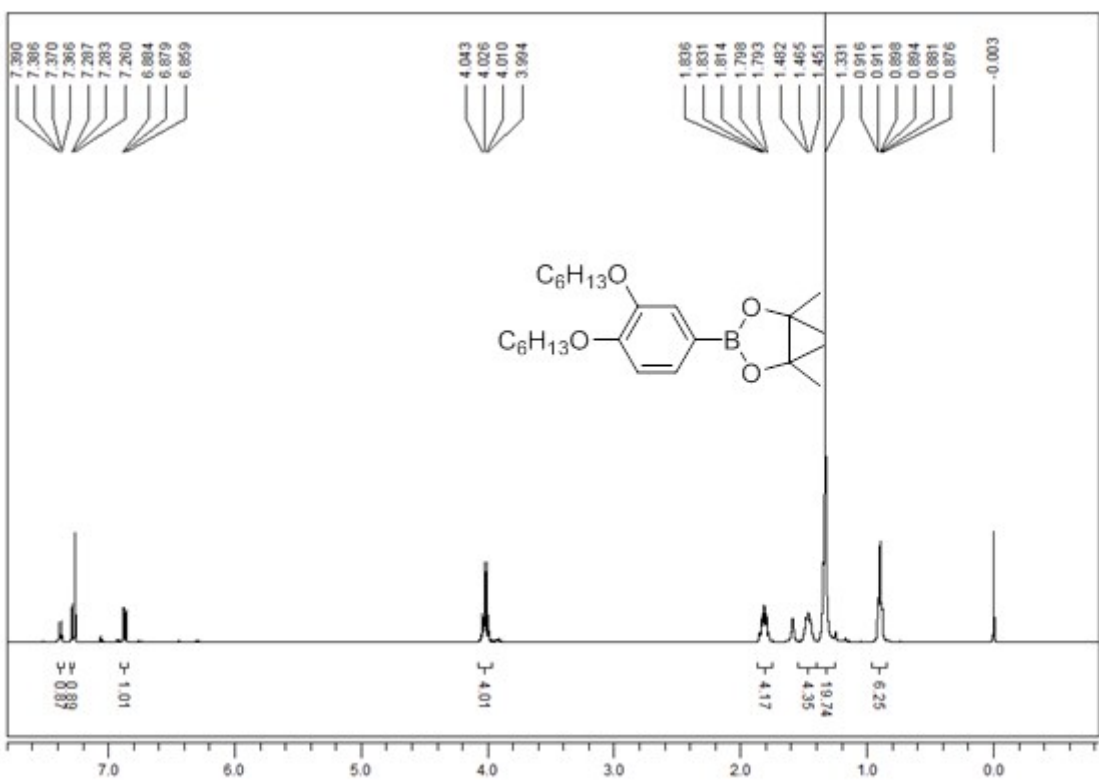


Figure S15. ^1H NMR (CDCl_3 , 400 MHz) spectrum of 2-(3,4-bis(hexyloxy)phenyl)-4,4,5,5-tetramethyl-1,3,2-dioxaborolane

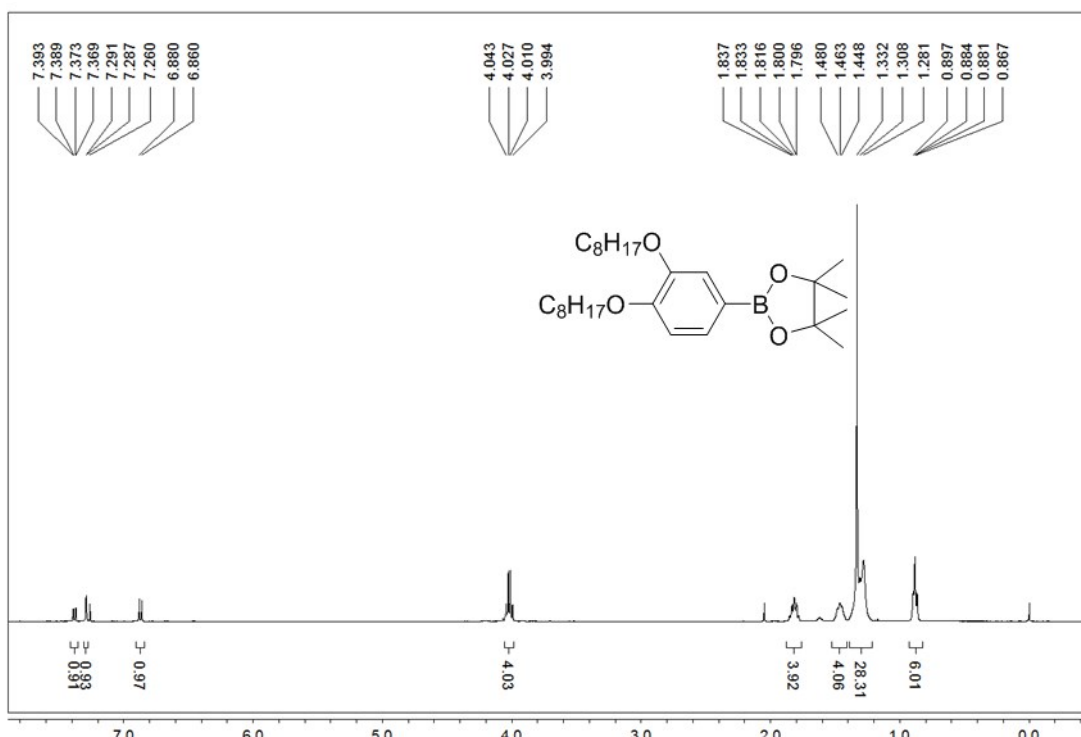


Figure S16. ^1H NMR (CDCl_3 , 400 MHz) spectrum of 2-(3,4-bis(octyloxy)phenyl)-4,4,5,5-tetramethyl-1,3,2-dioxaborolane

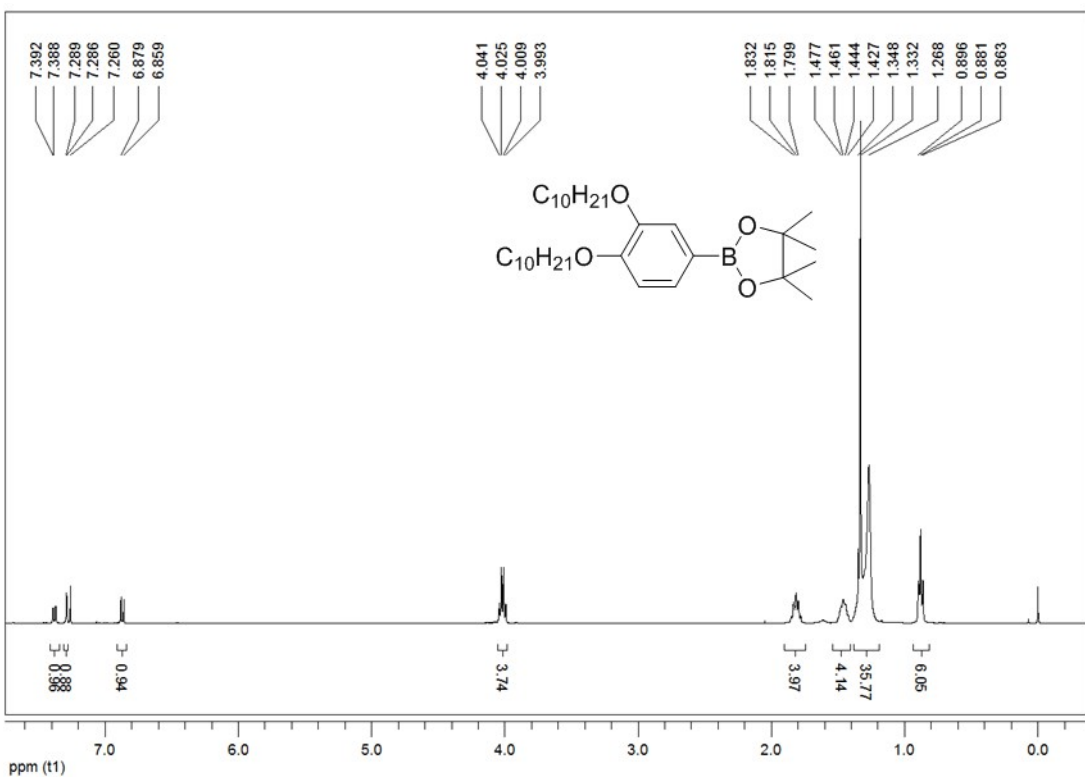


Figure S17. ^1H NMR (CDCl_3 , 400 MHz) spectrum of 2-(3,4-bis(decyloxy)phenyl)-4,4,5,5-tetramethyl-1,3,2-dioxaborolane

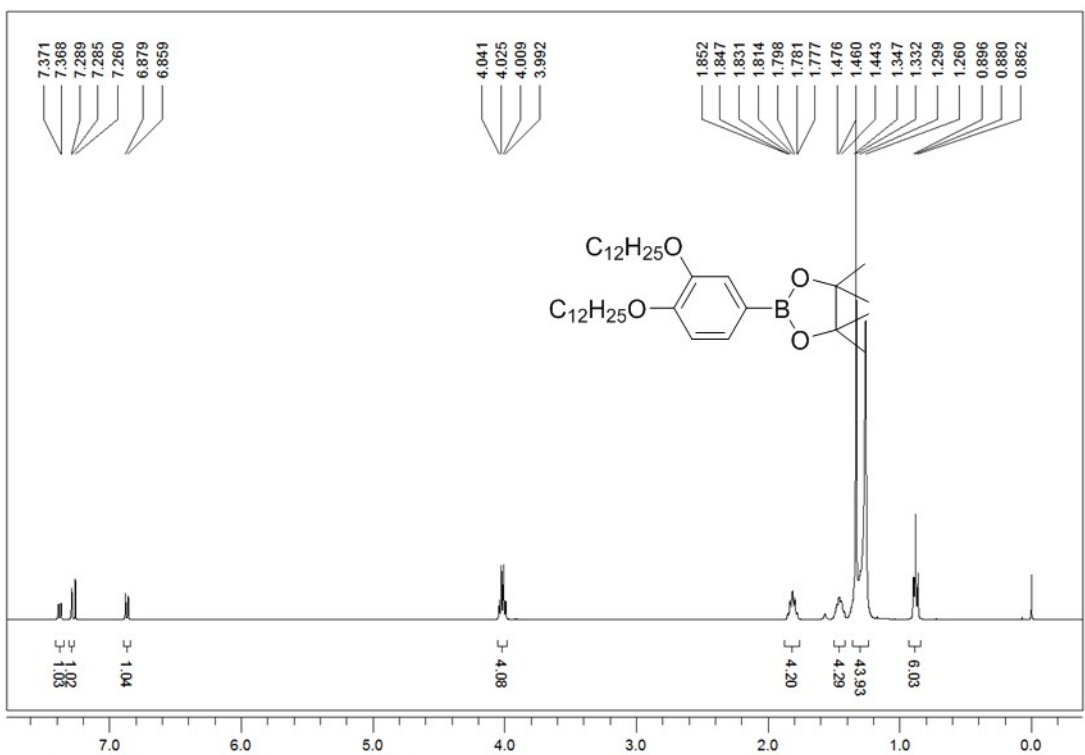


Figure S18. ^1H NMR (CDCl_3 , 400 MHz) spectrum of 2-(3,4-bis(dodecyloxy)phenyl)-4,4,5,5-tetramethyl-1,3,2-dioxaborolane

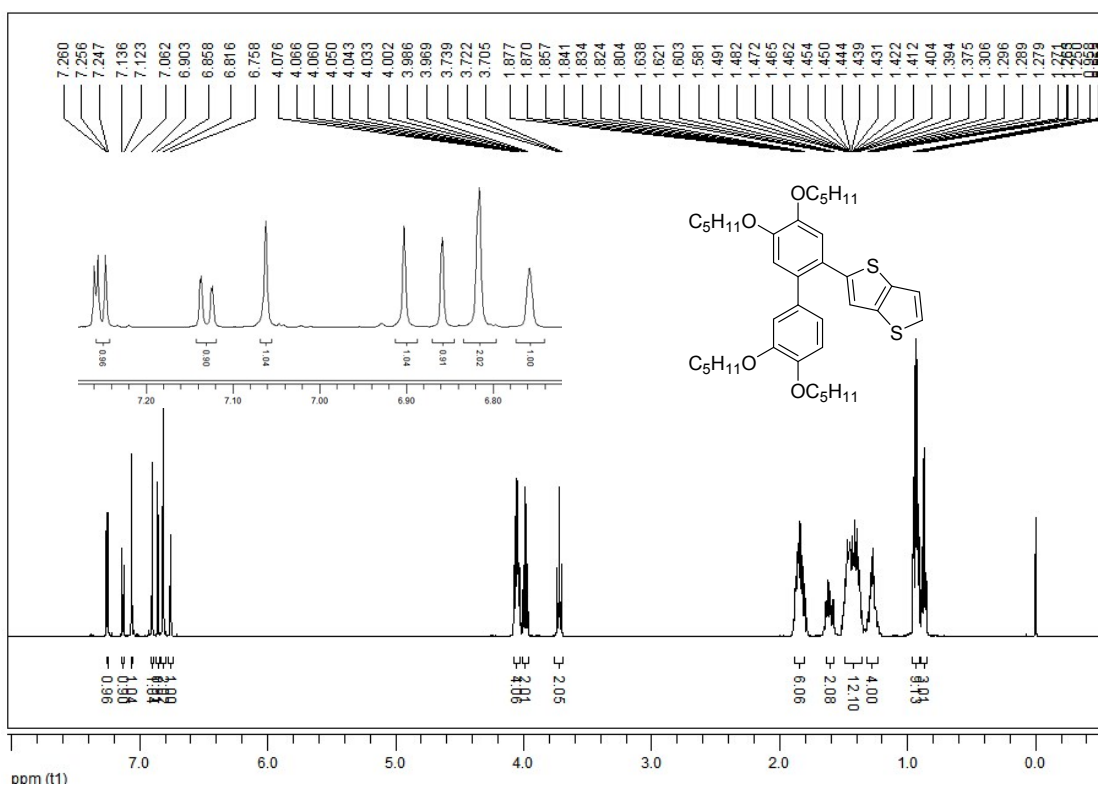


Figure S19. ¹H NMR (CDCl₃, 400 MHz) spectrum of **1-2**

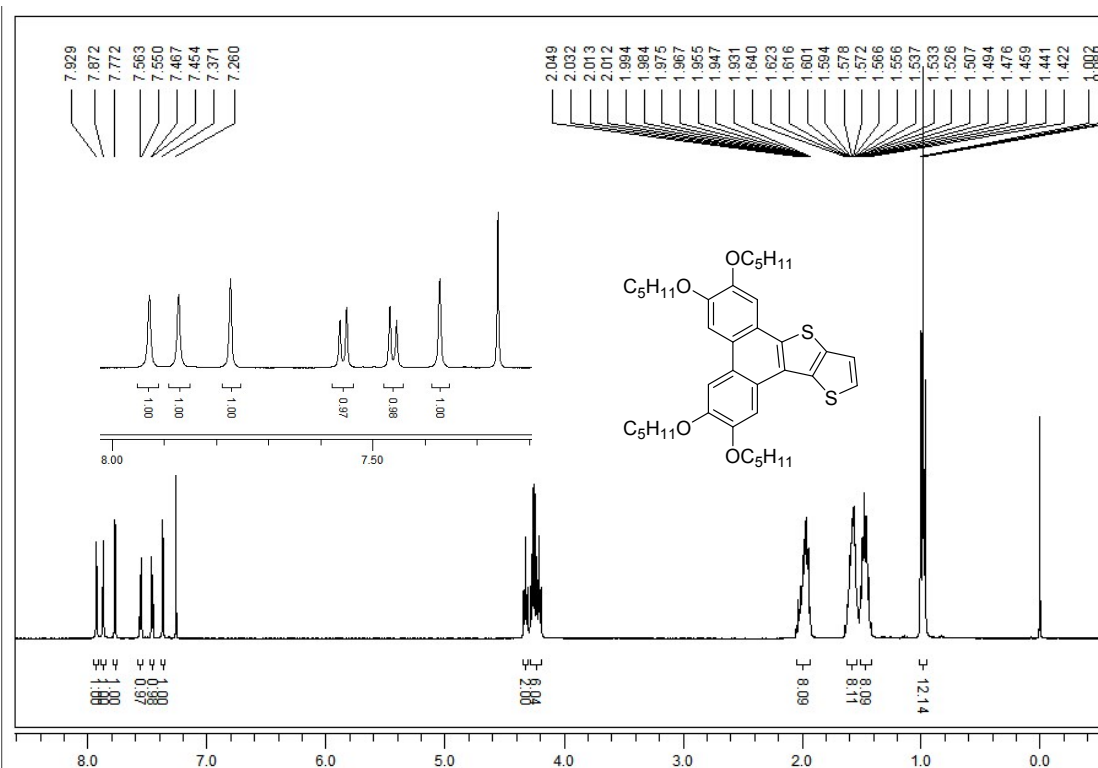


Figure S20. ¹H NMR (CDCl₃, 400 MHz) spectrum of **1-3**

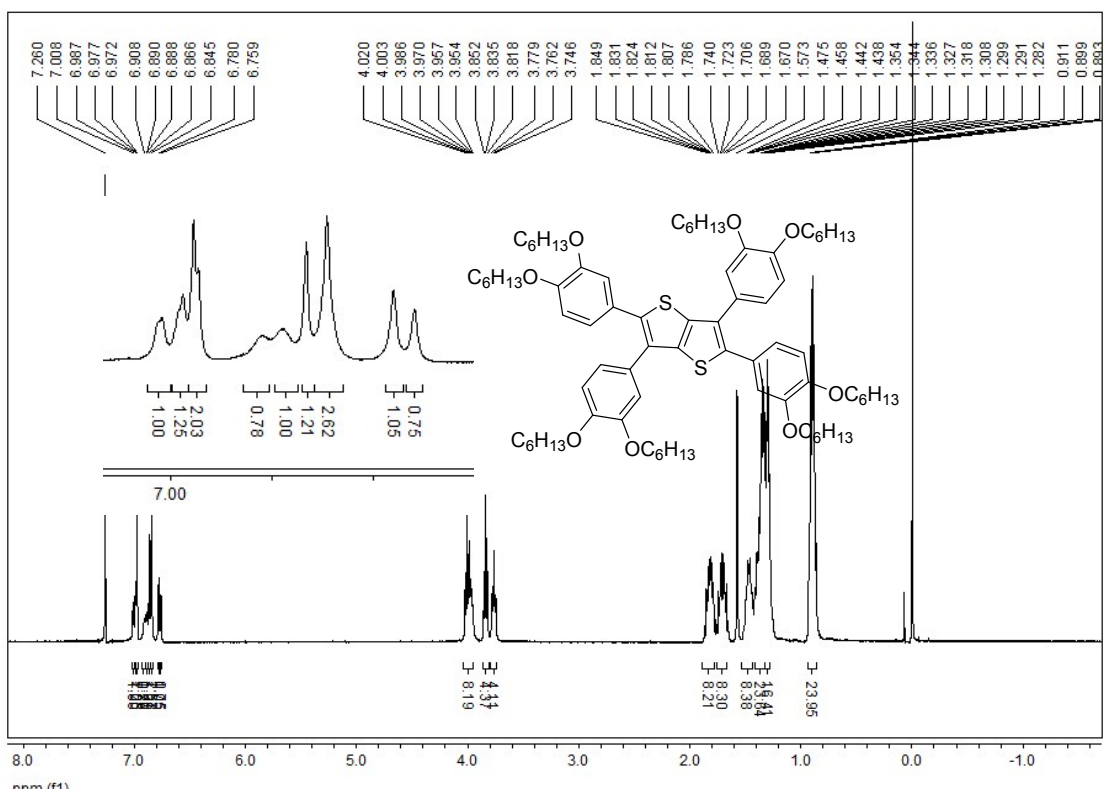


Figure S21. ¹H NMR(CDCl₃,400 MHz) spectrum of **D2**

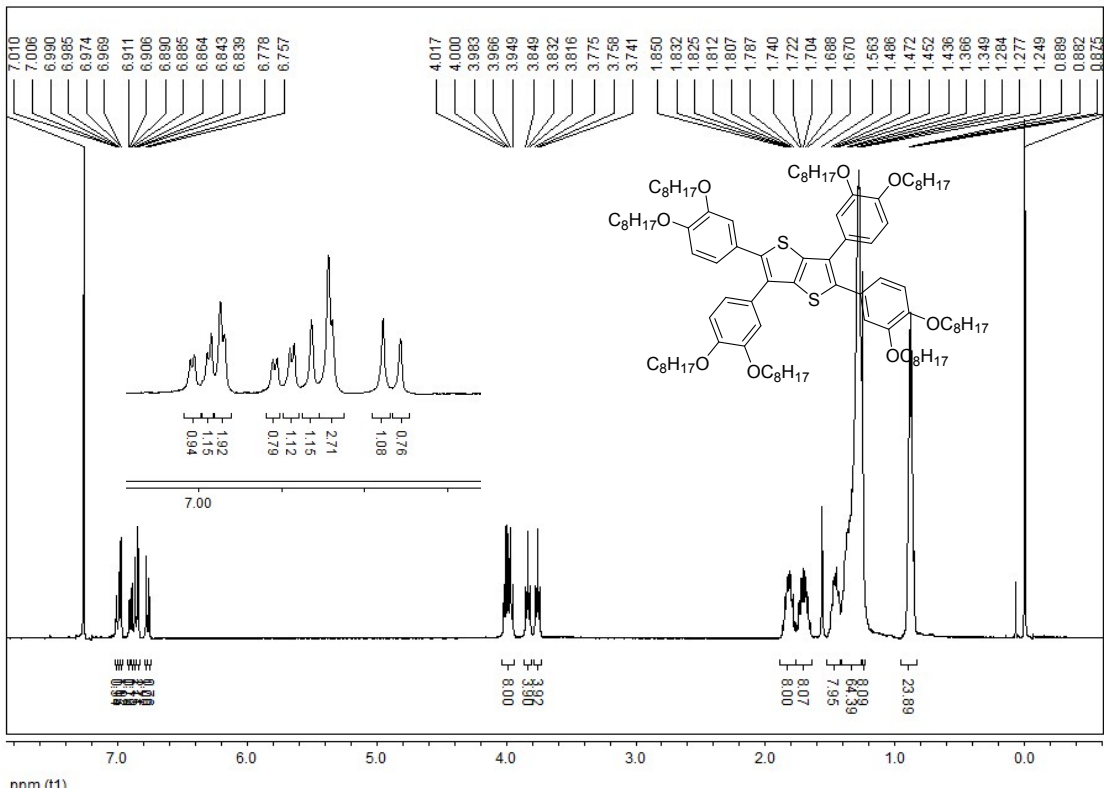


Figure S22. ¹H NMR (CDCl₃,400 MHz) spectrum of **D3**

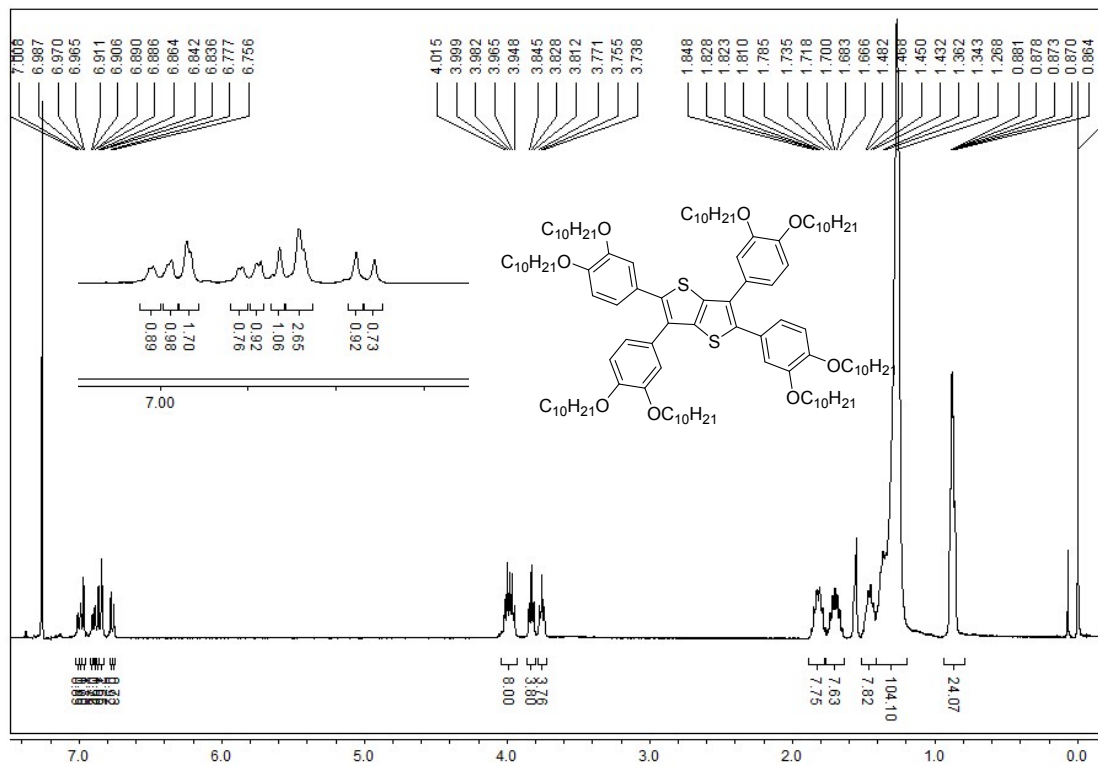


Figure S23. ^1H NMR (CDCl_3 , 400 MHz) spectrum of D4

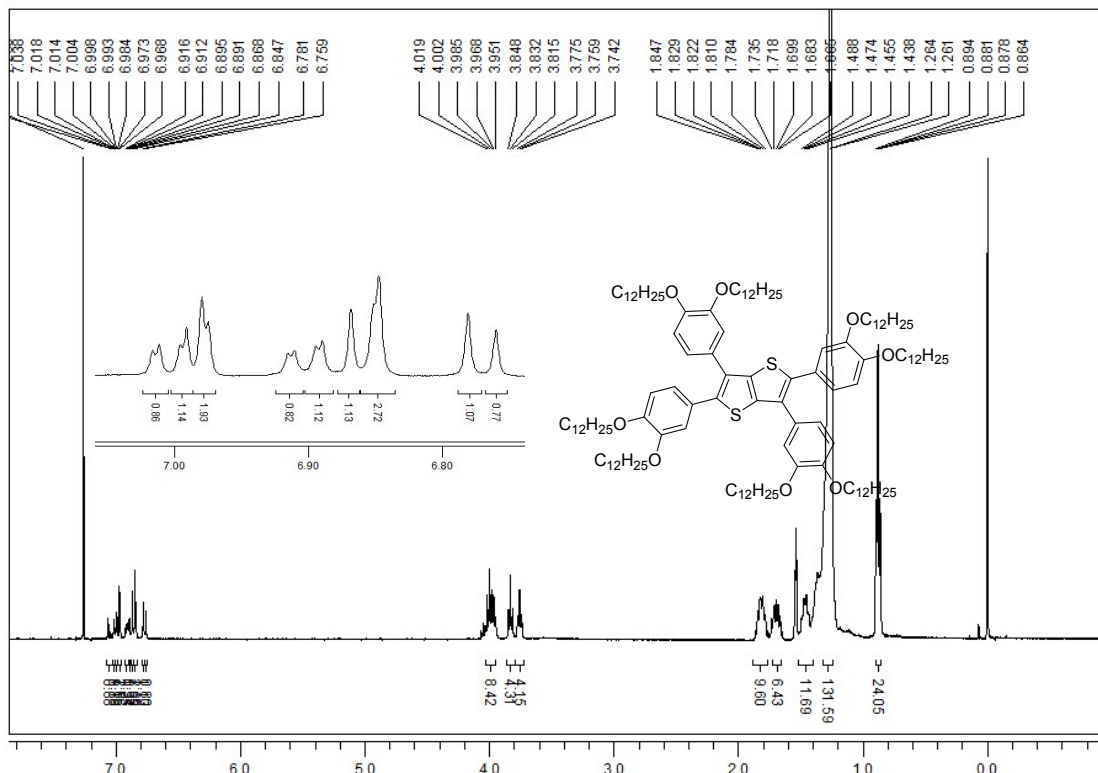


Figure S24. ^1H NMR (CDCl_3 , 400 MHz) spectrum of **D5**

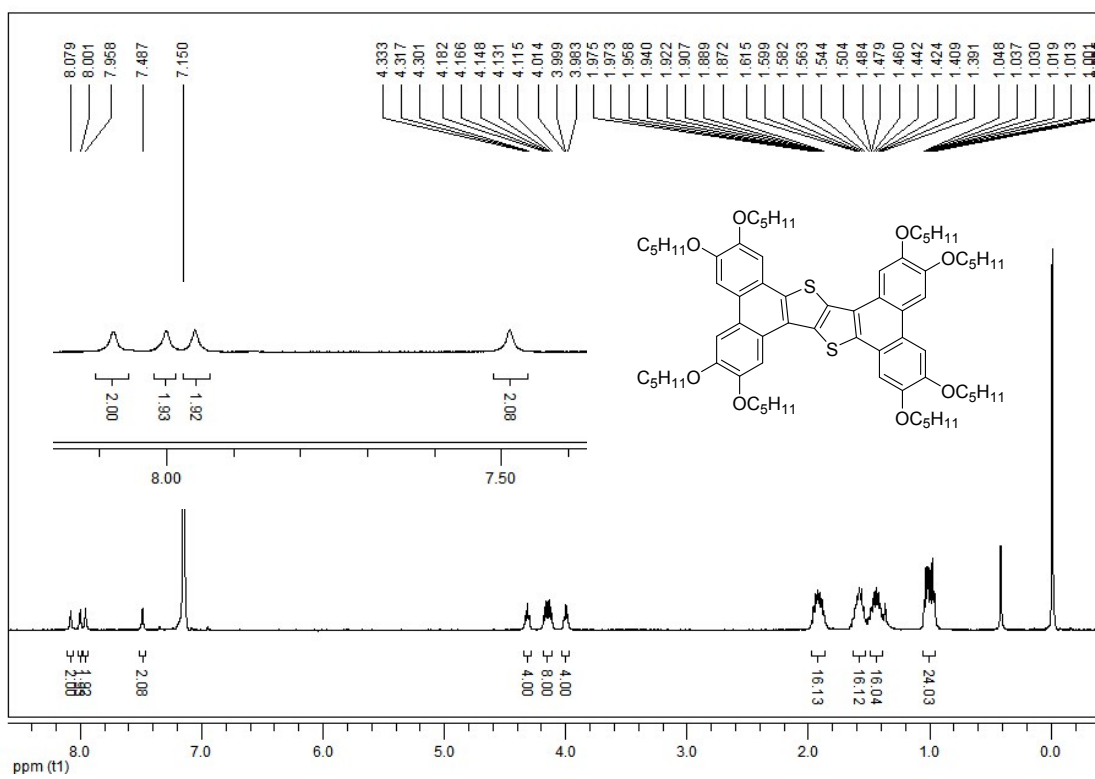


Figure S25. ^1H NMR (CDCl_3 , 400 MHz) spectrum of **M1**

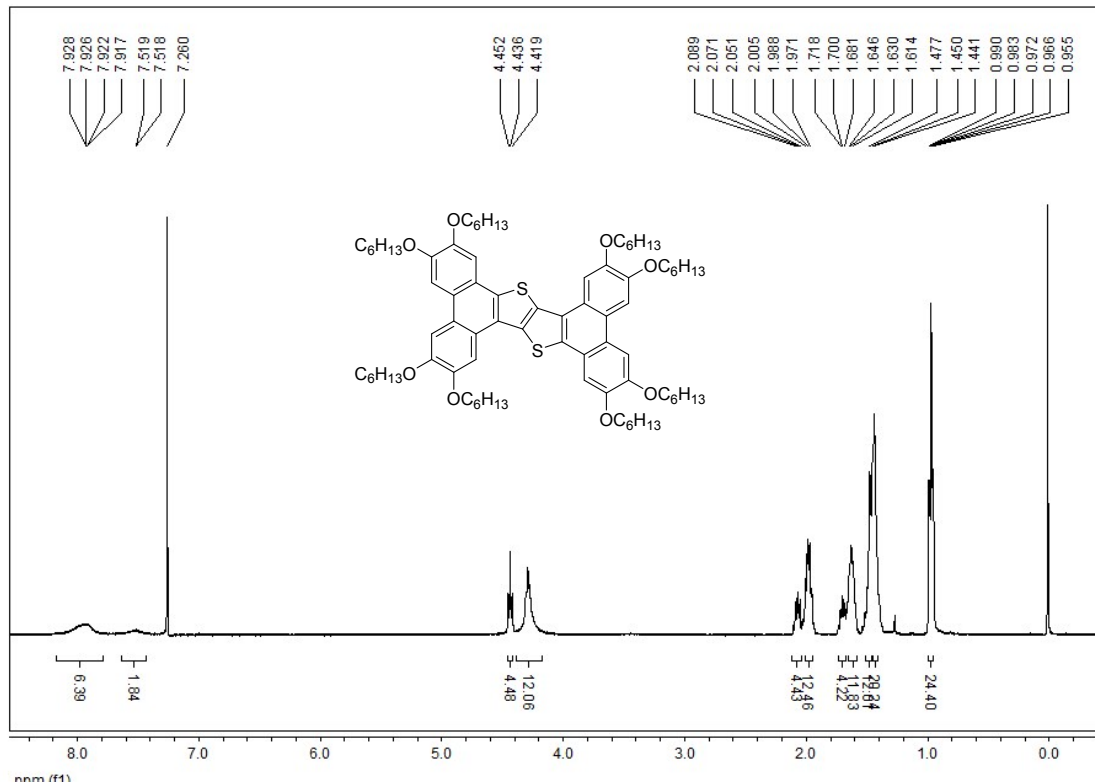


Figure S26. ^1H NMR (CDCl_3 , 400 MHz) spectrum of **M2**

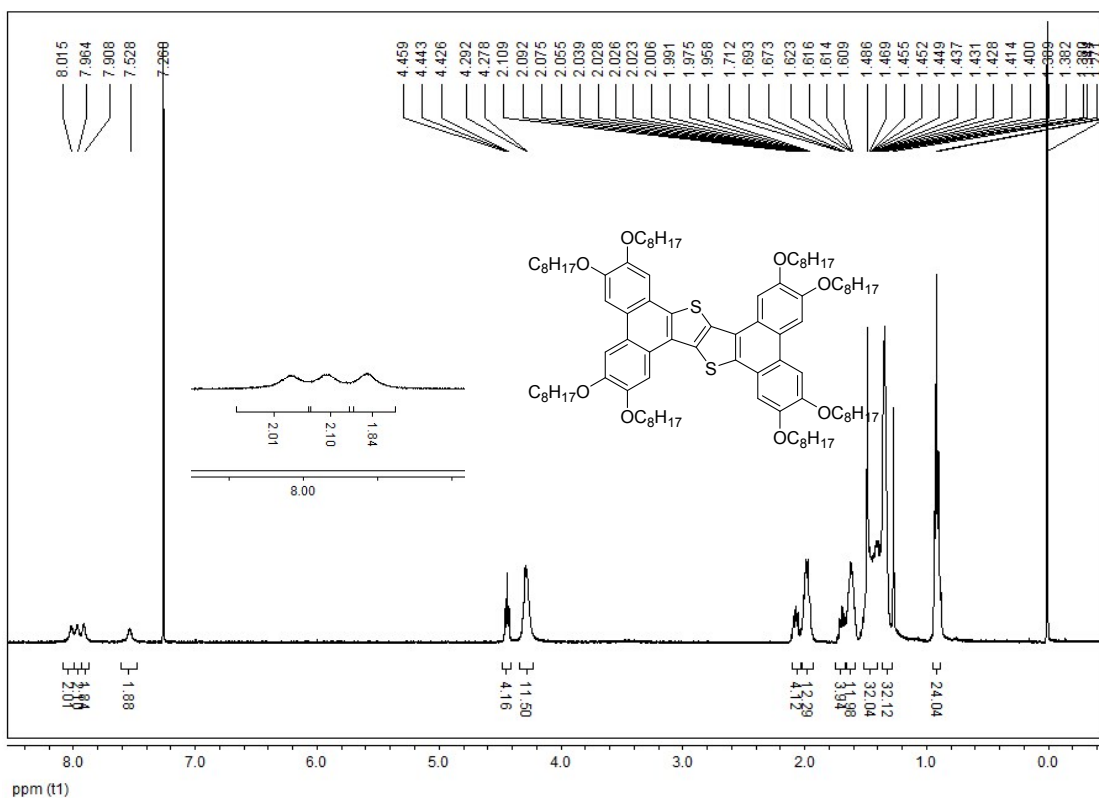


Figure S27. ^1H NMR (CDCl_3 , 400 MHz) spectrum of **M3**

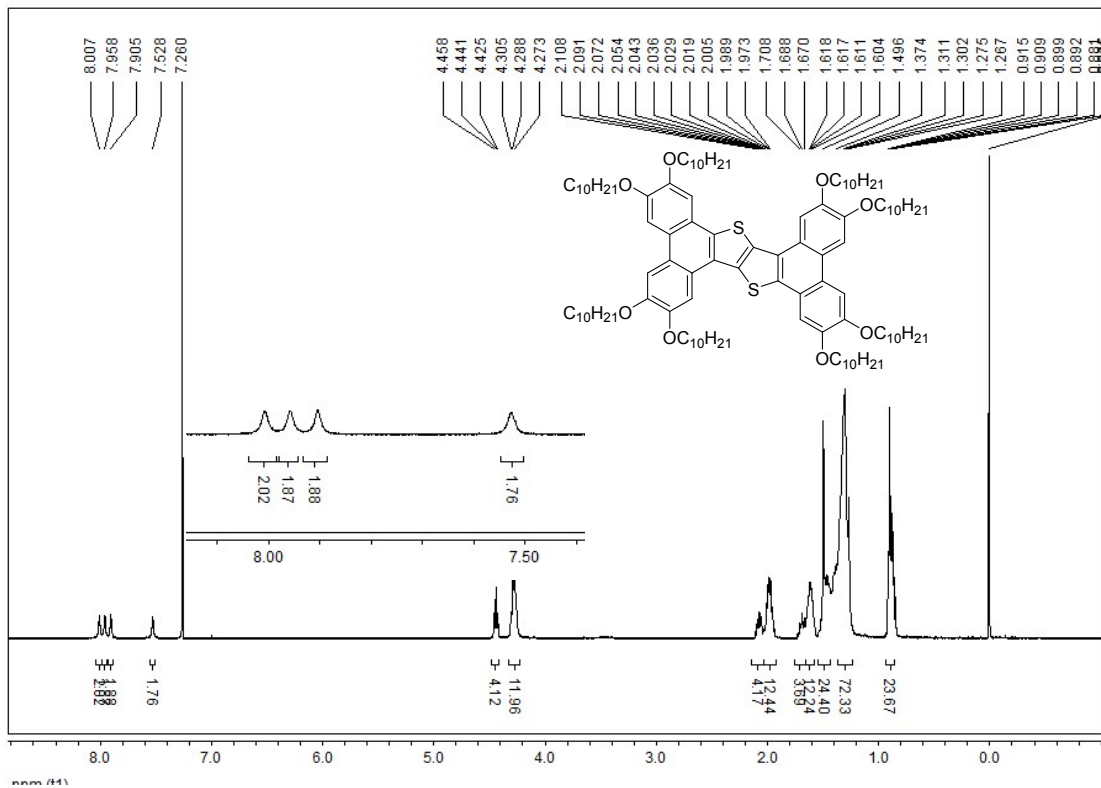


Figure S28. ^1H NMR (CDCl_3 , 400 MHz) spectrum of **M4**

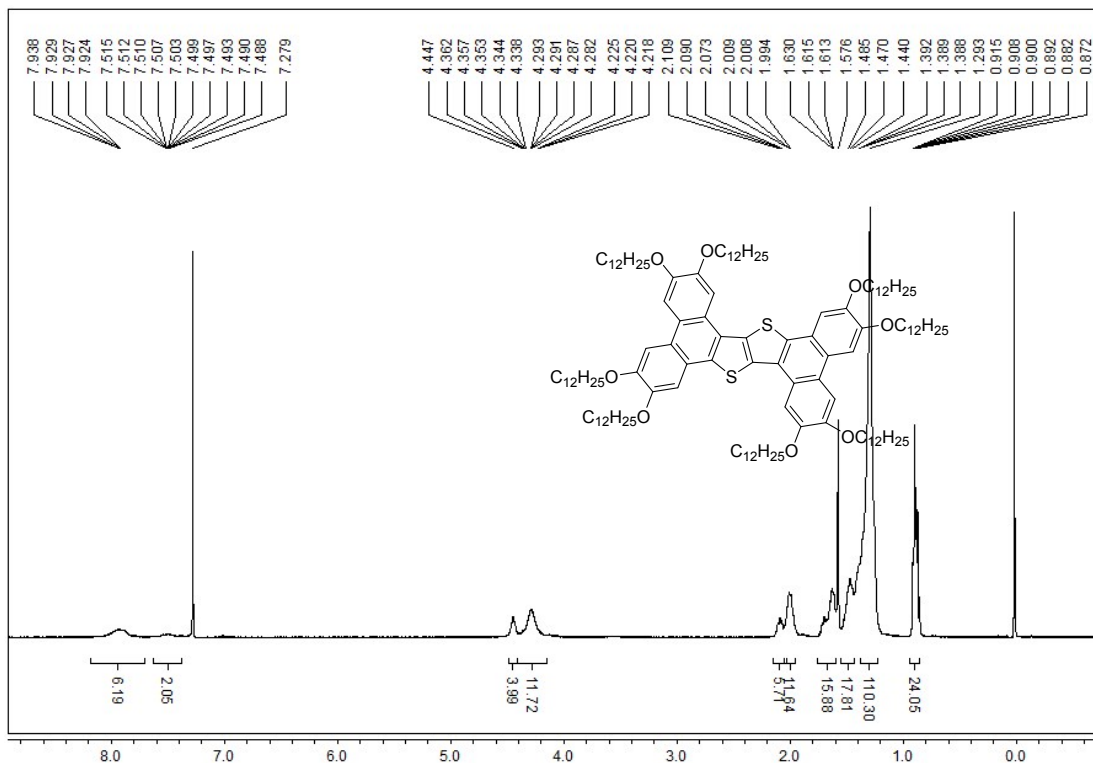


Figure S29. ¹H NMR (CDCl₃, 400 MHz) spectrum of M5

8. HRMS

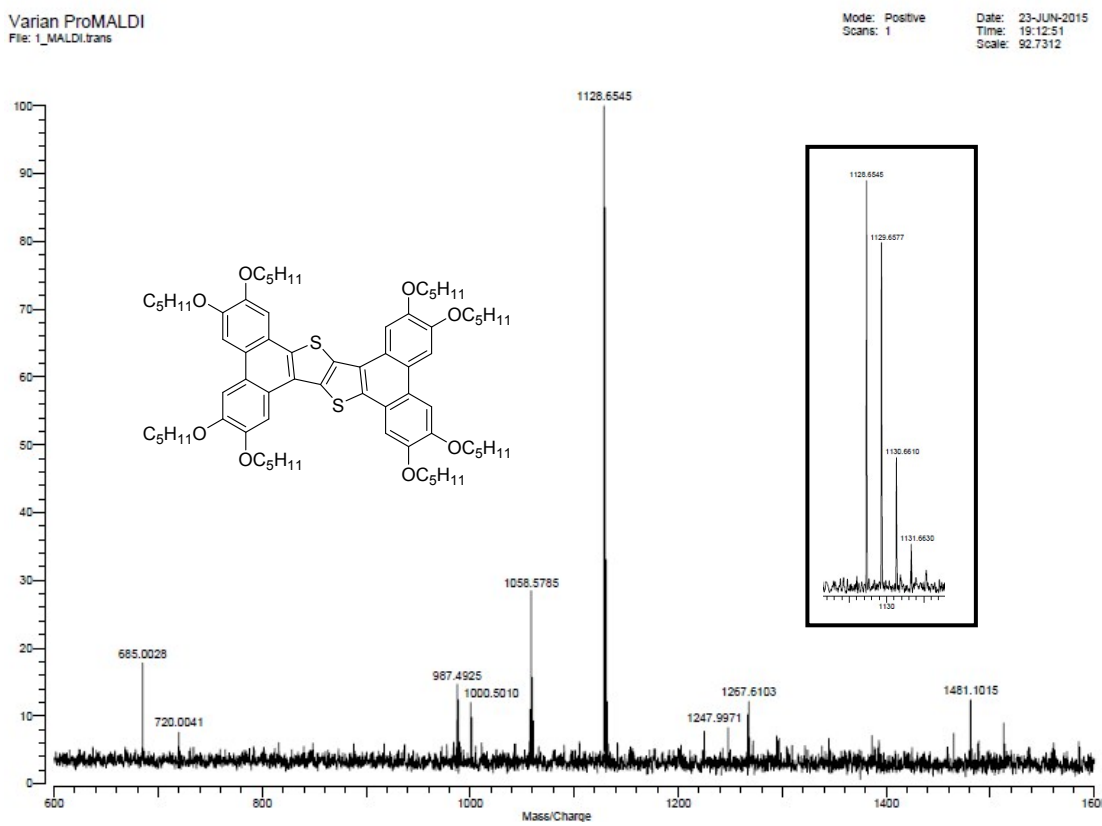


Figure S30. HRMS m/z (ESI) spectrum of M1

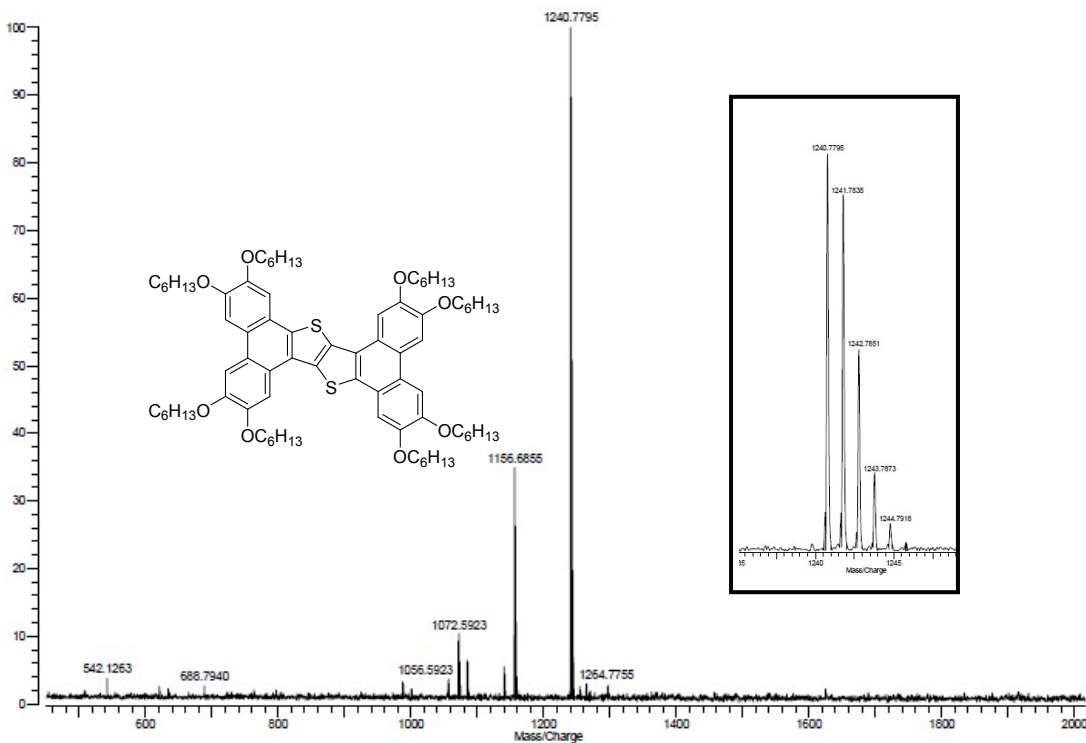


Figure S31. HRMS m/z (ESI) spectrum of M2

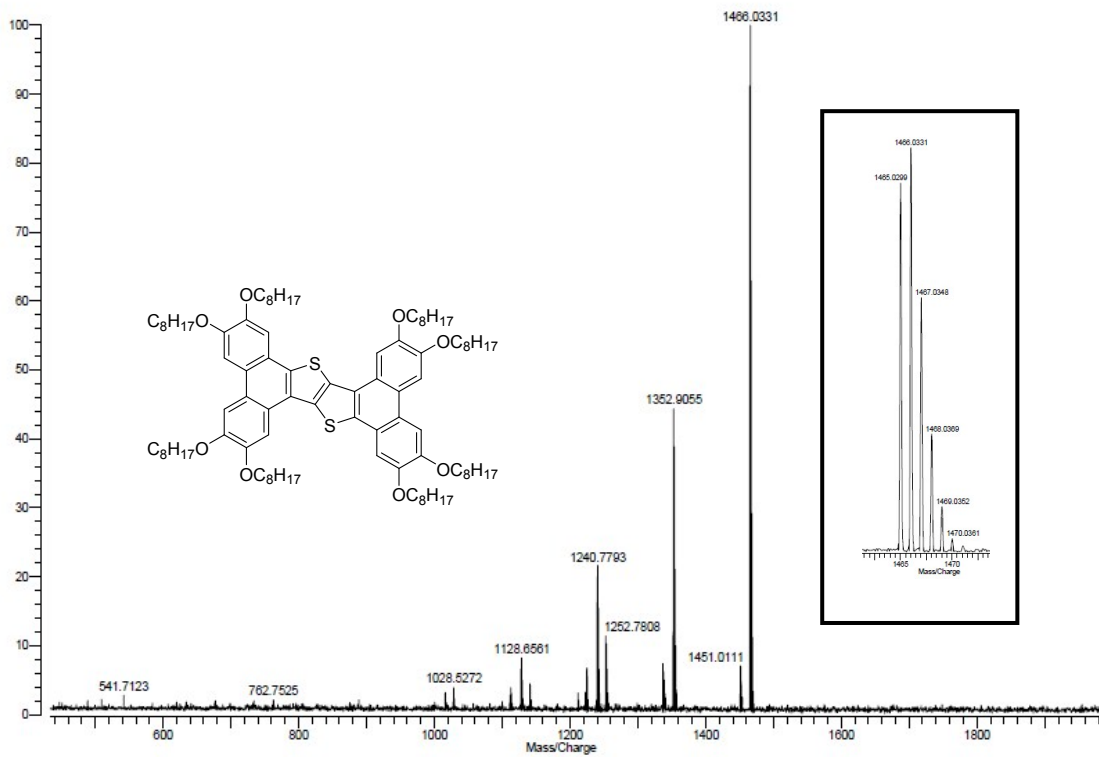


Figure S32. HRMS m/z (ESI) spectrum of M3

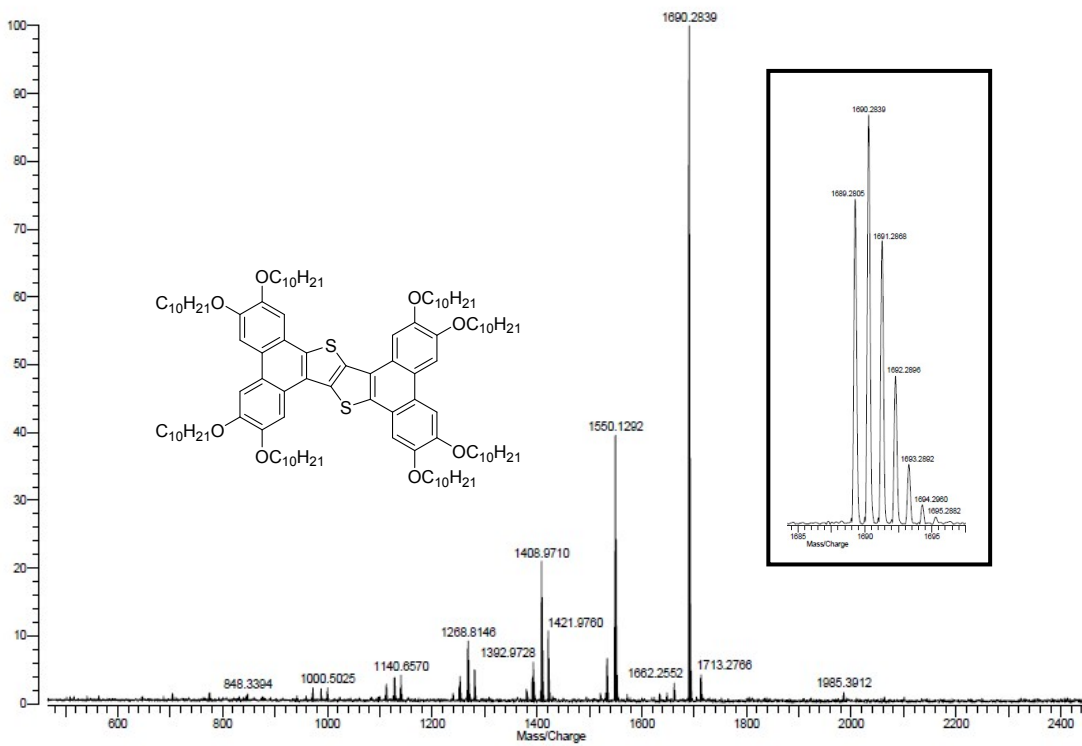


Figure S33. HRMS m/z (ESI) spectrum of M4

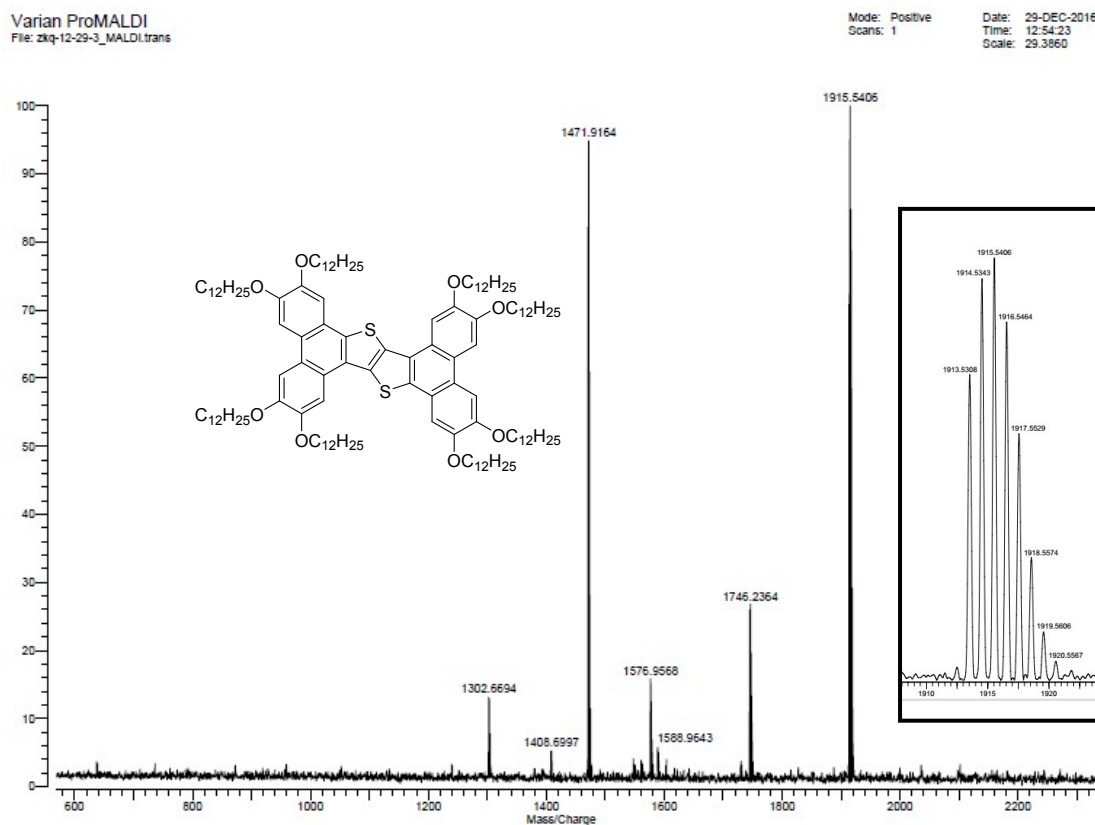


Figure S34. HRMS m/z (ESI) spectrum of M5